RadioGraphics

# Soft Tissue Tumors of the Head and Neck: Imaging-based Review of the WHO Classification[1]

*Ahmed Abdel Razek, MD • Benjamin Y. Huang, MD*

**CME FEATURE**

*See www.rsna.org/education/rg_cme.html*

**LEARNING OBJECTIVES FOR TEST 4**

*After completing this journal-based CME activity, participants will be able to:*

- Use the 2002 WHO classification system to characterize soft tissue tumors of the head and neck.
- Describe imaging features of several benign and malignant soft tissue tumors of the head and neck.
- Identify clinical and imaging parameters that help differentiate soft tissue tumors of the head and neck.

**TEACHING POINTS**

*See last page*

The World Health Organization (WHO) system for defining and classifying soft tissue tumors is usually applied to lesions that occur in the trunk and extremities, but it also provides an excellent framework for characterizing nonepithelial extraskeletal tumors of the head and neck. Although nonepithelial extraskeletal tumors are in the minority among head and neck lesions, they are by no means rare. The WHO classification system recognizes nine major types based on histologic differentiation: adipocytic, fibroblastic or myofibroblastic, fibrohistiocytic, smooth muscle, skeletal muscle, vascular, pericytic, and chondro-osseous tumors, as well as soft tissue tumors of uncertain differentiation. Tumors of each histologic type may be further subclassified on the basis of their biologic behavior as benign, intermediate (ie, having malignant potential), or malignant. Imaging plays an important role in the noninvasive diagnosis and characterization of nonepithelial soft tissue tumors of the head and neck, providing clues about tumor grade, composition, extent, and involvement of adjacent structures. Although the imaging characteristics of many such tumors are nonspecific, consideration of the clinical history in concert with the imaging findings may help limit the differential diagnosis or even allow reliable diagnosis of some of these tumors.



**Abbreviations:** ADC = apparent diffusion coefficient, FDG = fluorine 18 fluorodeoxyglucose, FNA = fine-needle aspiration, HIV = human immunodeficiency virus, SE = spin-echo, STIR = short inversion time inversion-recovery, WHO = World Health Organization

**RadioGraphics 2011;** 31:1923–1954 • **Published online** 10.1148/rg.317115095 • **Content Codes:** HN NR OI

[1]From the Diagnostic Radiology Department, Mansoura Faculty of Medicine, Elgomheryia St, Mansoura, Egypt 35512 (A.A.R.); and Department of Radiology, University of North Carolina, Chapel Hill, NC (B.Y.H.). Presented as an education exhibit at the 2010 RSNA Annual Meeting. Received April 19, 2011; revision requested May 24 and received July 26; accepted July 29. For this journal-based CME activity, the authors, editor, and reviewers have no relevant relationships to disclose. **Address correspondence to** A.A.R. (e-mail: *arazek@mans.edu.eg*).

## Introduction

Soft tissue tumors are a heterogeneous group of benign and malignant lesions that develop from various nonepithelial, extraskeletal elements, including adipose tissue, smooth and skeletal muscle, tendon, cartilage, fibrous tissue, blood vessels, and lymphatic structures. Although soft tissues constitute a large proportion of the human body (12%), soft tissue tumors account for fewer than 1% of all tumors. The annual incidence of soft tissue tumors is approximately 300 per 100,000 people in the general population, with benign lesions exceeding malignant ones by roughly 100 times. Although most soft tissue tumors occur in the trunk and extremities, the head and neck also are frequently involved. In fact, head and neck sarcomas represent an estimated 15% of sarcomas in adults and 35% of sarcomas in children (1–6).

Teaching Point

In the most recent World Health Organization (WHO) system for classification of soft tissue tumors, which was published in 2002, soft tissue tumors are grouped into nine major categories based on their predominant histologic makeup: adipocytic tumors, fibroblastic or myofibroblastic tumors, so-called fibrohistiocytic tumors, smooth muscle tumors, skeletal muscle tumors, vascular tumors, perivascular tumors, chondro-osseous tumors, and tumors of uncertain differentiation (7).

Clinical, pathologic, and radiologic differentiation of soft tissue tumors is often difficult because they frequently manifest as painless, enlarging masses and share many histologic and MR imaging features. Nonetheless, differentiation is important because the prognosis and therapeutic strategy differ according to the tumor type (2,6,8–12). Soft tissue tumors of the head and neck are frequently evaluated with imaging before biopsy or surgical resection is performed. The radiologists who interpret these imaging studies should be familiar with the spectrum of soft tissue tumors that occur in this region and with specific imaging features that may allow the diagnosis of certain types of soft tissue tumors.

The article reviews the WHO system for classification of soft tissue tumors and describes the imaging characteristics of several types of soft tissue tumors of the head and neck. Features that can help narrow the differential diagnosis of a soft tissue mass in the neck are discussed in detail.

## Biologic Behavior of Soft Tissue Tumors in the WHO Classification System

In addition to their classification on the basis of tissue type, as described above, soft tissue tumors are further subdivided according to their biologic behavior into benign tumors, intermediate tumors (those having malignant potential), and malignant tumors. Benign tumors are almost always cured with complete local excision and do not usually recur locally after resection; when they do recur, they are nondestructive (7).

Teaching Point

One of the major changes in the 2002 update of the WHO classification system was the introduction of two distinct subtypes of intermediate tumors with malignant potential: those with the potential for local invasion, and those with the potential for distant metastasis. Tumors in the first subcategory often recur locally after resection and show an infiltrative and focally destructive growth pattern; however, these lesions do not demonstrate the potential to metastasize. Lesions in the second subcategory are often locally aggressive but also have demonstrated a rare (probability, <2%) but well-documented ability to produce distant metastases (7).

In addition to having the potential for local destruction and recurrence, malignant tumors are associated with a significant risk (usually, at least 20%) for distant metastases (7). Table 1 shows an abbreviated summary of the WHO system for classifying soft tissue tumors on the basis of tissue type and biologic potential.

## Imaging Evaluation

### Computed Tomography

Computed tomography (CT) is often the first diagnostic imaging examination performed in patients in whom the presence of a head and neck mass is either evident or suspected. Current-generation CT scanners with multidetector arrays allow the acquisition of image datasets with isotropic resolution, from which multiplanar thin-section images and three-dimensional images can be reconstructed. CT examinations should be performed with intravenous iodinated contrast material unless there is a contraindication to its use (eg, iodine allergy). Typically, contrast material is injected at a rate of 2–4 mL/sec. A scan delay of 30–80 seconds follows the injection. After scanning in the axial plane, we typically perform

**Table 1**
**Summary of WHO Classification of Soft Tissue Tumors of the Neck**

| Histologic Type | Benign | Intermediate, Locally Aggressive | Intermediate, Rarely Metastasizing | Malignant |
|---|---|---|---|---|
| Adipocytic | Lipoma and its variants (lipoblastoma, hibernoma, lipomatosis) | Atypical lipomatous tumor, well-differentiated liposarcoma | … | Liposarcoma |
| Fibroblastic/myofibroblastic | Fibromatosis colli, myofibroma, giant cell angiofibroma | Desmoid-type fibromatosis | Solitary fibrous tumor, hemangiopericytoma, inflammatory myofibroblastic tumor (inflammatory pseudotumor) | Fibrosarcoma |
| So-called fibrohistiocytic | Benign fibrous histiocytoma, diffuse-type giant cell tumor (pigmented villonodular synovitis) | … | Giant cell tumor of soft tissues | Malignant fibrous histiocytoma (undifferentiated pleomorphic sarcoma) |
| Skeletal muscle | Rhabdomyoma | … | … | Rhabdomyosarcoma |
| Smooth muscle | Leiomyoma, angioleiomyoma | … | … | Leiomyosarcoma |
| Vascular | Hemangioma, lymphangioma | Kaposiform hemangioendothelioma | Kaposi sarcoma | Angiosarcoma |
| Perivascular | Glomus tumor, myopericytoma | … | … | Malignant glomus tumor |
| Chondro-osseous | Soft tissue chondroma | … | … | Mesenchymal chondrosarcoma, extraskeletal osteosarcoma |
| Uncertain differentiation | Myxoma | … | Ossifying fibromyxoid tumor | Synovial sarcoma, alveolar soft part sarcoma, primitive neuroectodermal tumor, Ewing sarcoma |

Source.—Reference 7.

two-dimensional multiplanar reconstruction to obtain images in the axial, sagittal, and coronal planes. Although it does not provide the soft tissue contrast resolution obtainable with magnetic resonance (MR) imaging, CT provides valuable information. Certain distinguishing CT characteristics (eg, the patterns of lesion mineralization, degree of attenuation, and involvement in adjacent bone, and the degree and pattern of vascularity) may be suggestive of a specific diagnosis (13).

## MR Imaging

We recommend that MR imaging be performed in all patients in whom the presence of a soft tissue tumor of the head and neck is suspected. MR imaging has superior soft tissue contrast resolution, which allows excellent characterization of the internal architecture and extent of tumors. A head or neck coil should be used,

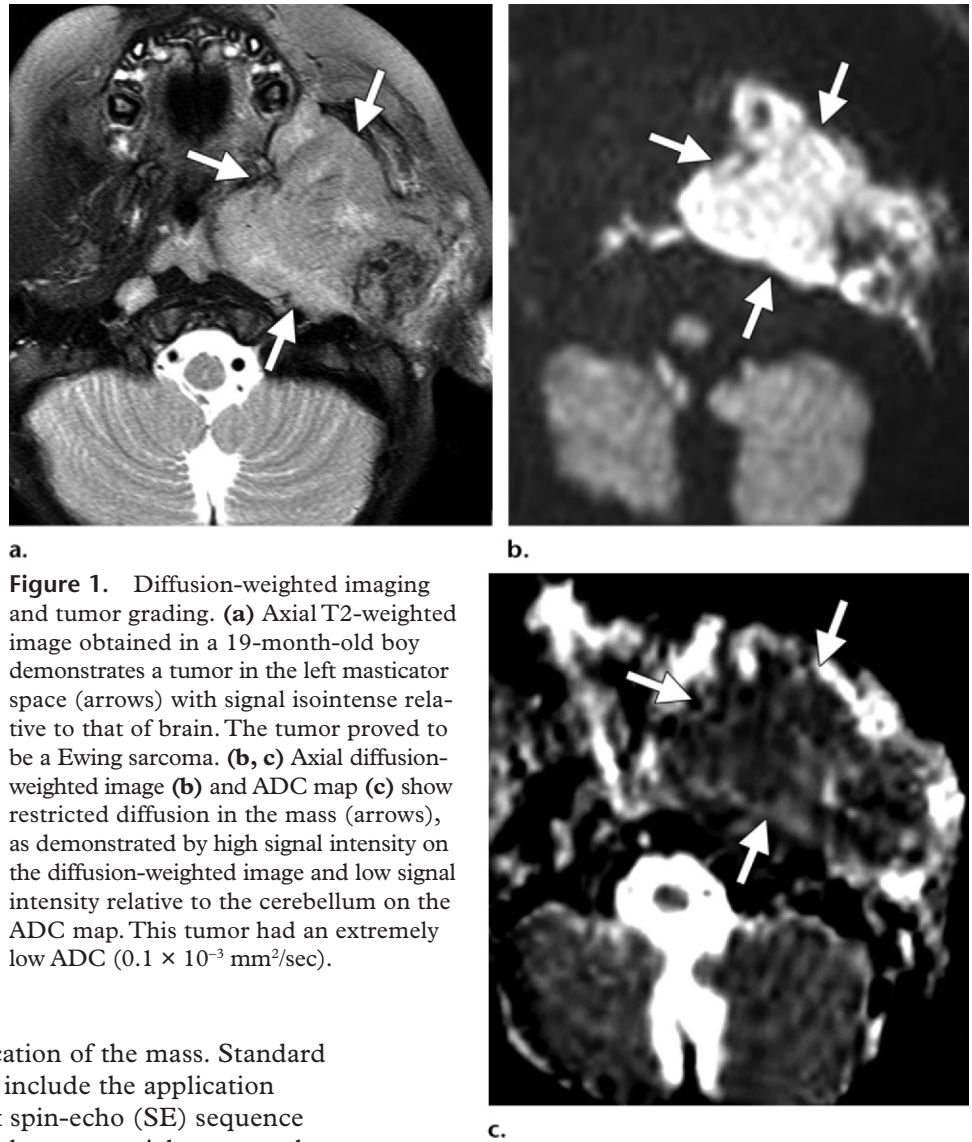


**Figure 1.** Diffusion-weighted imaging and tumor grading. **(a)** Axial T2-weighted image obtained in a 19-month-old boy demonstrates a tumor in the left masticator space (arrows) with signal isointense relative to that of brain. The tumor proved to be a Ewing sarcoma. **(b, c)** Axial diffusion-weighted image **(b)** and ADC map **(c)** show restricted diffusion in the mass (arrows), as demonstrated by high signal intensity on the diffusion-weighted image and low signal intensity relative to the cerebellum on the ADC map. This tumor had an extremely low ADC ($0.1 \times 10^{-3}$ mm$^2$/sec).

depending on the location of the mass. Standard examinations should include the application of a T2-weighted fast spin-echo (SE) sequence in axial and coronal planes, an axial or coronal fat-suppressed T2-weighted or short inversion time inversion-recovery (STIR) sequence, a T1-weighted standard SE or fast SE sequence in all three planes, and fat-saturated T1-weighted imaging with a gadolinium-based contrast material in all three planes.

Diffusion-weighted imaging also may play a role in characterizing head and neck masses. This modality has been used in the differentiation of malignant and benign tumors, because tumoral apparent diffusion coefficient (ADC) values tend to vary according to the stage of tumor cell differentiation, the degree of tumor cellularity, the presence of necrotic tissue, and the degree of degenerative change in interstitial tissues. Malignant soft tissue tumors usually have low ADC values, which are represented as low signal intensity on ADC maps, whereas benign tumors tend to have higher ADC values. In particular, it has been shown that the ADC correlates with tumor cellularity in soft tissue sarcomas and is lower in malignant nonmyxoid soft tissue tumors than in benign tumors (14–17). In one report, malignant nonmyxoid soft tissue tumors had a mean ADC of $0.94 \times 10^{-3}$ mm$^2$/sec (compared with $1.31 \times 10^{-3}$ mm$^2$/sec for benign nonmyxoid tumors) and ADC values that were all less than $1.35 \times 10^{-3}$ mm$^2$/sec (15). Unfortunately, there is substantial overlap in ADC values between benign and malignant soft tissue tumors, which limits the sensitivity of the technique for distinguishing between the two. Nonetheless, extremely low ADC values in soft

Teaching Point

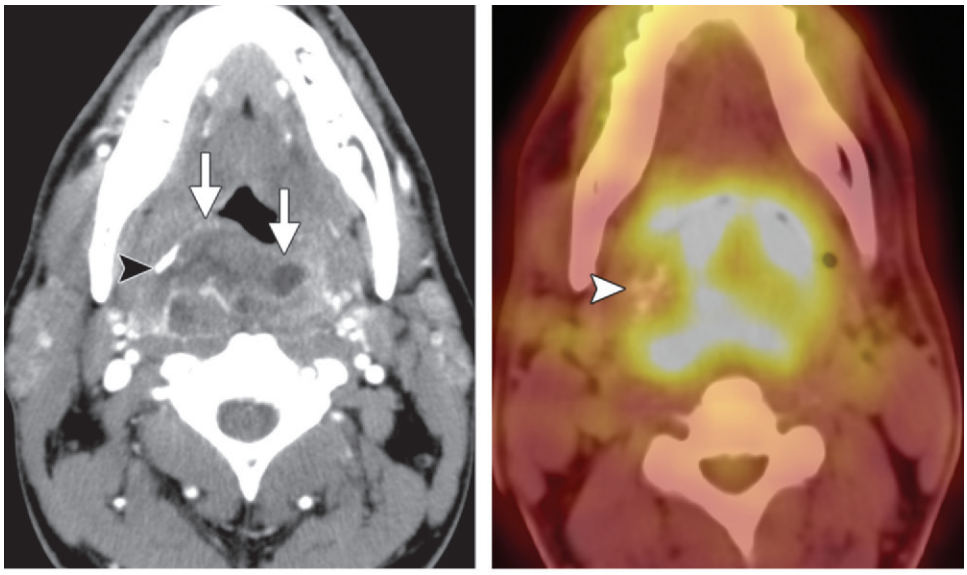

a. b.

**Figure 2.** FDG PET and soft tissue tumor grading. **(a)** Axial contrast-enhanced CT image in a 38-year-old man with difficulty swallowing demonstrates a heterogeneously enhancing posterior oropharyngeal mass (arrows) that also contains areas of nonenhancement. Note the calcification (arrowhead) in the right lateral aspect of the tumor. **(b)** Fused PET/CT image demonstrates high radiotracer uptake in the tumor (standardized uptake value, 4.6), a finding suggestive of high-grade sarcoma. Calcification (arrowhead) also is clearly identifiable. The tumor proved to be a synovial sarcoma.

tissue tumors (indicated qualitatively by very low signal intensity relative to nearby muscle or brain tissue on ADC maps) are highly suggestive of malignancy (Fig 1).

Dynamic contrast-enhanced MR imaging and dynamic susceptibility-weighted contrast-enhanced MR imaging also show promise for characterizing soft tissue tumors, because malignant tumors tend to show earlier and faster uptake of contrast material than benign tumors do. In one study performed with dynamic contrast-enhanced MR imaging, the rapidity of tumor enhancement was one of the parameters with the greatest power for identifying malignancy in soft tissue tumors, along with the presence of necrosis and cystic degeneration and the lesion size (18). At dynamic susceptibility-weighted contrast-enhanced MR imaging, a threshold dynamic susceptibility contrast ratio (percentage) of 30.7% is reported to be associated with accuracy of 84.6% for differentiating malignant from benign head and neck tumors (19).

## Positron Emission Tomography

Positron emission tomography (PET) performed with fluorine 18 fluorodeoxyglucose (FDG) is now widely used for grading and staging of head and neck tumors and for detection of local tumor recurrence. A number of studies have examined the diagnostic value of FDG PET for characterizing bone and soft tissue tumors. In one meta-analysis, the overall pooled sensitivity and specificity of FDG PET for detection of all sarcomas were 91% and 85%, respectively; for soft tissue sarcomas alone, the pooled sensitivity and specificity were 88% and 86%, respectively. Standardized uptake values in sarcomas (range, 0.80–15.43) were significantly higher than those in benign tumors (range, 0.22–1.43). Furthermore, high-grade sarcomas demonstrated significantly higher standardized uptake values (range, 2.59–14.7) than did low-grade sarcomas (range, 0.20–1.80) (20). Therefore, FDG PET can be useful in the preoperative grading of soft tissue tumors (Fig 2). However, it is important to keep in mind that although PET/CT and other physiologic imaging techniques such as diffusion-weighted MR imaging and dynamic contrast-enhanced MR imaging can be extremely useful for differentiating between malignant and benign soft tissue tumors, they do not generally allow a tissue-specific diagnosis.

## Tissue Sampling

Despite the utility of noninvasive imaging techniques for characterizing tumors in the head and neck, tissue sampling remains the reference standard for definitive diagnosis of soft tissue tumors. A percutaneous, incisional, or excisional biopsy should be performed in any head and neck tumor the diagnosis of which is in doubt after an adequate imaging work-up. Methods that may be used for tissue sampling include percutaneous fine-needle aspiration (FNA) biopsy, percutaneous core needle biopsy, and open incisional or excisional biopsy. Although open biopsy provides the greatest diagnostic accuracy, percutaneous biopsy methods are frequently used for the initial diagnosis of nonmucosal lesions because they are less invasive than open biopsy techniques. In the biopsy of nonpalpable, deep-seated lesions or lesions located near vital vascular or neural structures, imaging (CT or ultrasonography [US]) is typically used for guidance.

At FNA biopsy, cells are obtained for histologic analysis, but no information is gleaned about the tissue architecture or matrix. Nevertheless, with the use of ancillary analytic techniques (eg, immunohistochemical analysis, cytogenetic analysis, flow cytometry, and electron microscopy), FNA biopsy affords a sensitivity and specificity approaching 95% for the diagnosis of soft tissue malignancies, with reported false-positive and false-negative rates ranging from less than 1% to 4% for adequate specimens. However, FNA biopsy is not very useful for the definitive classification of soft tissue tumors, with success rates in this regard ranging from 50% to 70% (21). The accuracy of FNA biopsy for histologic subtyping was reported to be greater for pediatric sarcomas (92%) than for adult sarcomas (52%). Although histologic subtyping based on aspirates obtained at FNA biopsy is not possible in many cases, the information provided allows sufficiently reliable differentiation of malignant and benign soft tissue tumors to initiate definitive treatment in most cases (83% of soft tissue sarcomas in one report) (22). When possible, an on-site cytopathologist should be available for immediate interpretation and for determining the need for additional material for ancillary studies.

Core needle biopsy is often the next diagnostic step when initial FNA biopsy results are inconclusive or when more definitive tissue characterization is necessary before definitive treatment and the lesion cannot be easily extirpated. Unlike FNA biopsy, core needle biopsy can provide tissue samples in which the tumor matrix is included and the tissue architecture is preserved, two characteristics that are better for the purposes of histologic subtyping.

At percutaneous biopsy, regardless of the method used, the approach varies according to the location of the tumor in relation to vital structures. In general, the shortest path between the skin and the lesion should be chosen, and tissue should be taken from the solid contrast-enhancing portions of the tumor; cystic, necrotic, or calcified components should be avoided (23,24). One limitation of needle biopsies is that the tissue samples are small and are obtained at focal points within the tumor; thus, clinically significant areas may be missed and the results of analysis may not be representative of the overall character of the tumor (20).

## Features allowing Differentiation of Soft Tissue Tumors

Differentiating the many types of soft tissue tumors, or even distinguishing between benign and malignant tumors, is often extremely difficult with imaging alone. In addition to imaging findings, pertinent clinical data must be taken into account; these data might include the age of the patient, the rapidity of onset and duration of the mass, the presence of pain, the presence of other medical conditions, and a history of traumatic injury or irradiation at the site of the tumor. Multiplicity of tumors, locations of tumors, and characteristic imaging features of tumors (eg, calcification, MR signal intensity, and vascularity) also can help limit the differential diagnosis.

### Patient Demographics and Clinical History

Clinical and demographic data should always be taken into account when interpreting imaging studies. The patient's age can be an important discriminatory factor in the differential diagnosis. Certain benign entities (eg, infantile hemangioma, lymphangioma, lipoblastoma, fibromatosis colli, and myofibroma) occur primarily in young children, as do malignant tumors such as rhabdomyosarcoma. Hibernoma, desmoid-type fibromatosis, synovial sarcoma, and Ewing sarcoma occur primarily in adolescents and young adults, whereas lesions such as liposarcoma and malignant fibrous histiocytoma occur primarily in older adults.

**Table 2**
**Imaging Features Suggestive of Soft Tissue Tumor Malignancy**

| |
|---|
| Large volume |
| Extracompartmental extension |
| Poorly defined margins |
| Broad interface with underlying fascia |
| Inhomogeneous MR signal intensity |
| High signal intensity on T2-weighted MR images |
| Invasion of bone or neurovascular structures |
| Intratumoral hemorrhage |
| Intratumoral necrosis |
| Marked, primarily peripheral enhancement |

Note.—Adapted, with permission, from reference 1.

The specificity of the diagnosis can be further improved by considering the clinical manifestations. Painless, slow-growing, long-standing masses are likely to be benign, whereas the presence of pain or a rapid increase in the size of a mass are worrisome signs of possible malignancy (25). The patient's medical history also may provide clues to the diagnosis. For example, a calcified mass at a site of previous traumatic injury is suggestive of myositis ossificans. Alternatively, a mass at a site that was previously irradiated should arouse concern about the possibility of radiation-induced sarcoma, particularly if the mass occurs years after the completion of radiation therapy. In one study, the average latency period between irradiation for treatment of nasopharyngeal carcinoma and development of a secondary sarcoma in the head and neck was 9 years, with actual intervals ranging broadly from 3 to 26 years (26). In that study, the most common histologic subtypes of radiation-induced sarcoma were fibrosarcoma (41.5%), osteosarcoma (22.6%), and malignant fibrous histiocytoma (13.2%); other subtypes, including rhabdomyosarcoma, angiosarcoma, and chondrosarcoma, occurred rarely.

Teaching Point

In some cases, the presence of a predisposing condition or concomitant lesions may provide clues to the diagnosis. For example, desmoid-type fibromatosis is seen in association with Gardner syndrome, and myxomas associated with fibrous dysplasia are seen in Mazabraud syndrome.

## Lesion Morphologic Characteristics

The likelihood that a lesion is malignant is increased by the presence of certain conventional imaging features (Table 2). Although the relative sensitivity and specificity of any single feature is low, the probability of malignancy increases with the number of suspicious features present (1). In general, a lesion size of more than 5 cm and a location deep to fascia are characteristics that are often associated with malignancy. Lesion size of less than 3 cm, lobulated or smooth well-defined margins, and a superficial location are suggestive of benignity.

## Lesion Location and Number of Lesions

Some tumors are most frequently found in a particular region of the head or neck. For instance, fibromatosis colli exclusively involves the sternocleidomastoid muscle, whereas pigmented villonodular synovitis involves the temporomandibular joint. Lesions usually affecting the orbits include inflammatory pseudotumor, giant cell angiofibroma, and rhabdomyosarcoma. Soft tissue tumors that frequently arise in the sinonasal cavities include many sarcomas (fibrosarcoma, rhabdomyosarcoma, malignant fibrous histiosarcoma, leiomyosarcoma), solitary fibrous tumors, and sinonasal glomus tumors. Some tumors have a predilection for certain anatomic compartments, such as skin (dermatofibroma, dermatofibrosarcoma), subcutaneous tissues (lipoma, nodular fasciitis), intermuscular (synovial sarcoma, lipoma, myositis ossificans) and intramuscular (lipoma, pleomorphic sarcoma, liposarcoma, rhabdomyosarcoma) compartments, and meninges (solitary fibrous tumor, hemangiopericytoma) (6).

In addition, depending on the clinical context, a multiplicity of lesions may be suggestive of multiple hemangiomas, multifocal infantile myofibromatosis, or multiple desmoid tumors. Finally, infiltrative, transspatial lesions may represent sarcomas, lipomas, hemangiomas, or lymphangiomas.

## Calcification

The presence of calcification in a soft tissue lesion occasionally helps establish its histologic type. Mineralization of the soft tissue may be due to matrix calcification or ossification. The presence of calcified matrix within a lesion should lead to a focus on chondro-osseous–type tumors in the differential diagnosis. Linear and spiculated calcification and amorphous central calcification are seen in osteosarcomas, whereas stippled and curvilinear calcifications are typical of cartilaginous tumors, such as soft tissue

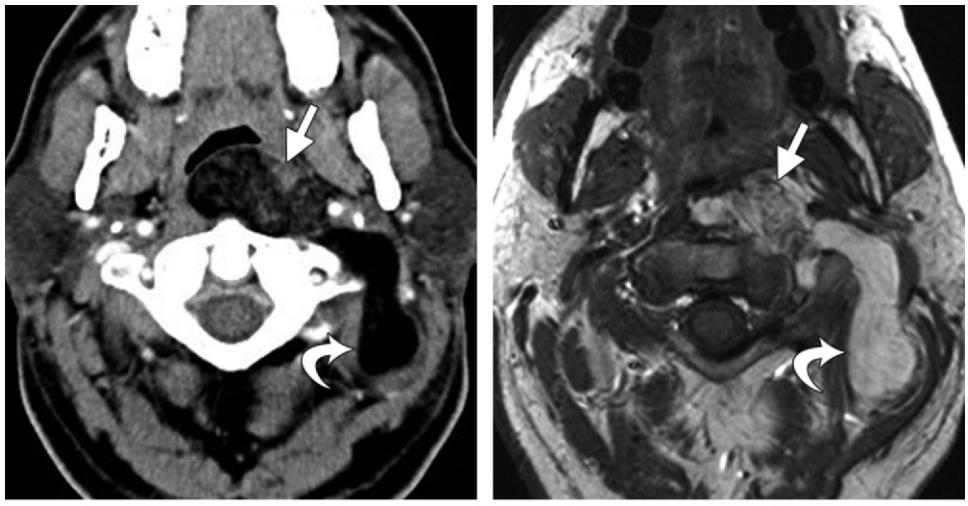

a. b.

**Figure 3.** Intramuscular lipoma. Axial contrast-enhanced CT scan **(a)** and unenhanced T1-weighted MR image **(b)** obtained in a 49-year-old man demonstrate a soft tissue mass in which the signal intensity of fat predominates. The mass extends from the prevertebral region into the left perivertebral space (curved arrow). Although the appearance of the left paraspinal portion is typical of lipoma, nonadipose elements within the prevertebral portion (straight arrow) make it difficult to exclude well-differentiated liposarcoma from the differential diagnosis. The mass proved to be an intramuscular lipoma with interspersed degenerate skeletal muscle fibers. The nonadipose elements did not enhance at MR imaging after the administration of contrast material (not shown).

chondroma and chondrosarcoma. Peripheral calcification can be seen in myositis ossificans and ossifying fibromyxoid tumors. Other tumors that may become calcified include lipoma, liposarcoma, malignant fibrous histiocytoma, synovial sarcoma, and rhabdomyosarcoma.

### Imaging Appearance and Enhancement Pattern

Lesion signal intensity on MR images and contrast enhancement on CT scans and MR images occasionally provide helpful clues to the diagnosis. A region of low signal intensity on T2-weighted MR images may represent hemosiderin deposition, calcification, or fibrous tissue. A low-signal-intensity lesion in the region of the temporomandibular joint is highly suggestive of pigmented villonodular synovitis, which is characterized by hemosiderin deposition. Similarly, tumors containing calcification (eg, chondrosarcoma, osteosarcoma, myositis ossificans) typically demonstrate areas of low signal intensity on T2-weighted images. Tumors containing fibrous tissue (eg, desmoid-type fibromatosis, leiomyosarcoma, fibrosarcoma) also may demonstrate signal hypointensity relative to the signal intensity in muscle, although not all fibrous tumors do so (5).

Predominance of fatty signal intensity within a lesion should lead to a differential diagnostic focus on adipocytic tumors, whereas the presence of multiple regions that are void of signal or that show intense contrast enhancement steers the diagnosis toward highly vascularized tumors such as giant cell angiofibroma, hemangiopericytoma, sinonasal glomus tumor, and other vascular soft tissue tumors. Angiofibroma, desmoid-type fibromatosis, angioleiomyoma, and hemangiopericytoma tend to demonstrate marked enhancement.

Generally speaking, malignant lesions tend to show more marked and more rapid enhancement than benign lesions do. In addition, heterogeneous enhancement, particularly in association with areas of necrosis, is suggestive of malignancy (5). However, in most cases, enhancement characteristics alone cannot be used to reliably distinguish between benign and malignant lesions.

## Adipocytic Tumors

Adipocytic tumors are the largest group of mesenchymal soft tissue tumors, mostly because of the high prevalence of lipomas and angiolipomas (7). Benign adipocytic processes include lipoma and variants thereof: lipomatosis, lipoblastoma,

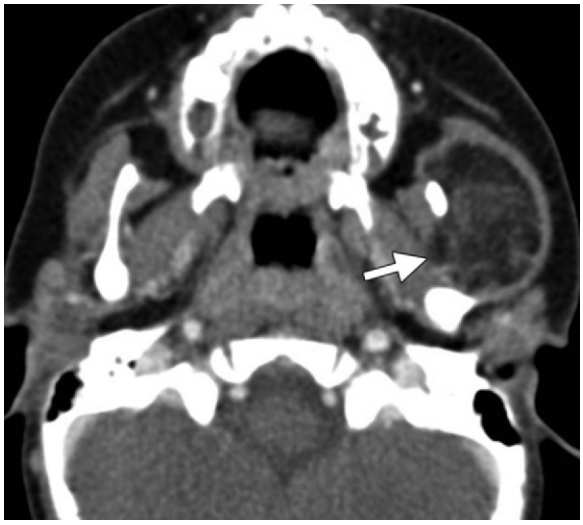

**Figure 4.** Lipoblastoma. Axial contrast-enhanced CT scan obtained in an 18-month-old child demonstrates a well-circumscribed, predominantly fatty mass with internal septation and nonadipose soft tissue components (arrow) centered in the left masseter muscle. Although the tumor is indistinguishable from a low-grade liposarcoma, the patient's age helps establish the diagnosis of lipoblastoma.

and hibernoma. Liposarcomas, of which there are many histologic subtypes, are malignant adipocytic tumors. Well-differentiated liposarcoma and atypical lipomatous tumor are locally aggressive lesions with intermediate malignant potential (7,27).

## Lipoma

Teaching Point

Lipomas are the most common mesenchymal tumors, accounting for roughly 16% of soft tissue tumors. Approximately 25% of lipomas occur in the head and neck, mostly in subcutaneous locations at the posterior aspect of the neck. They rarely develop in the anterior aspect of the neck, infratemporal fossa, oral cavity, larynx, tonsil, parotid area, hypopharynx, nasopharynx, or retropharyngeal space.

Lipomas are composed of mature adipocytes with a small proportion of surrounding or intervening connective tissue stroma. They can be differentiated from normal fatty deposits by their internal architecture, their mass effect on adjacent structures, and their metabolic behavior. Most are well-defined encapsulated masses found just beneath the skin or between muscles and other connective-tissue structures. The imaging characteristics of classic lipomas, which are well described in the literature, include attenuation equivalent to that of subcutaneous fat on CT images and high signal intensity matching that of fat on both T1- and T2-weighted MR images. On fat-suppressed images, the signal within lipomas drops out completely. Thin septa occasionally can be seen within the tumors, but simple lipomas rarely present a diagnostic challenge (27–29).

Numerous histopathologic variants of lipoma have been described. These include fibrolipoma, osteolipoma, chondrolipoma, intramuscular lipoma, angiolipoma, chondroid lipoma, spindle cell lipoma, pleomorphic lipoma, and sialolipoma. These variants differ from simple lipoma both in regard to their clinical manifestations and their appearance at microscopy. Atypical features that may be seen include septa thicker than 2 mm, septal nodularity, and soft tissue components with the attenuation or signal intensity of muscle, fibrous tissue, hemorrhage, or calcification. These soft tissue components may demonstrate contrast enhancement (27–29). In such instances, it may be impossible to distinguish a variant lipoma from a liposarcoma on the basis of imaging appearance alone (Fig 3).

## Lipoblastoma

Lipoblastoma is a rare, rapidly growing, benign tumor that is seen in children younger than 3 years. Although these lesions are benign, they commonly recur after resection (14%–24%). Lipoblastomas contain collections of immature fat cells in varying stages of maturity with intervening septa that form lobules. The tumors are associated with chromosomal abnormalities at 8q11–q13. At CT, lipoblastomas are nonenhancing lesions containing areas with attenuation similar to that of fat (Fig 4). On T1-weighted MR images, the signal intensity of the tumors varies, depending on the maturity of the adipocytes, and may be hyperintense (mature adipocytes) or intermediate (immature adipocytes). On T2-weighted images, high signal intensity is seen in the lesion. The lesion contents typically appear heterogeneously fatty, with intermediate streaks and whorls of higher signal intensity attributable to the intralesional fibrous tissue framework. Unlike subcutaneous fat deposits, lipoblastomas exhibit high signal intensity on fat-suppressed images, a diagnostically specific characteristic (27,30). The imaging features of lipoblastoma overlap with those of well-differentiated liposarcoma (see the section on "Atypical Lipomatous Tumor [Well-differentiated Liposarcoma]"); however, patient age allows reliable differentiation of the two entities (3).

## Hibernoma

Hibernoma is a rare, benign, slow-growing tumor consisting of brown fat. It usually arises in regions in which vestiges of fetal brown fat persist (eg, the neck). Hibernomas usually occur in people between the ages of 20 and 40 years, with a slight predominance in females. The tumors are generally hypervascular and are characterized histologically by multivacuolar adipocytes and brown fat cells interspersed with univacuolar adipocytes. CT and MR images depict hibernoma as a well-demarcated mass with attenuation and signal intensity between that of subcutaneous fat and that of muscle. On fat-suppressed MR images, signal suppression in the tumor may be incomplete because of the nature and amount of the lipid content. Prominent enhancing vessels may be evident within hypervascular tumors, but the internal contrast enhancement of hibernomas varies (28,31). Although they are benign tumors, hibernomas notably demonstrate increased radiotracer uptake at FDG PET because of their brown fat content (32).

## Lipomatosis

Lipomatosis, a condition caused by diffuse overgrowth of mature adipocytes, usually affects children aged 2 years or younger but also may occur in adults. Various forms have been described, including infiltrating congenital lipomatosis of the face, encephalocraniocutaneous lipomatosis, and multiple symmetric lipomatosis or Madelung disease (29).

Infiltrating congenital lipomatosis of the face consists of infiltrative, nonencapsulated accumulations of mature fat cells, features that are typically limited to the face. Lesion growth may lead to facial asymmetry, parotid involvement, osseous hypertrophy, and macroglossia. The disease process may be associated with a cutaneous capillary blush and mucosal neuromas (29,33).

Encephalocraniocutaneous lipomatosis is an infiltrative lipomatous process that commonly affects the temporofrontal area unilaterally, including the cerebral tissues, leptomeningeal tissues, and skull; in some cases, the eye and the heart are also affected. Associated cerebral malformations and calcification may be seen (29).

Madelung disease is a rare condition characterized by the abnormal bilateral symmetric proliferation of adipose tissue in the head, neck, and shoulders. It mainly affects white men aged 25–60 years. These patients often have a history of alcohol abuse, and the condition may be associated with dyslipidemia, diabetes mellitus, hyperthyroidism, liver disease, hypertension, hyperuricemia, renal tubular acidosis, macrocytic anemia, and polyneuropathy. This disease has typical clinical and imaging appearances and is not difficult to diagnose. The distribution of the fatty deposits distinguishes Madelung disease from obesity (6,34).

## Atypical Lipomatous Tumor (Well-differentiated Liposarcoma)

Among the changes introduced in the 2002 WHO classification was the recognition that atypical lipomatous tumor and well-differentiated liposarcoma are essentially synonymous entities. These lesions are classified as locally aggressive tumors with intermediate malignant potential. On radiologic images, they may resemble lipomas in which more than 75% of the tissue volume consists of fat. There is extensive overlap between the characteristics of benign lipomatous tumors and those of well-differentiated liposarcomas, and noninvasive differentiation may be impossible. Features that may help distinguish well-differentiated liposarcomas include the patient's age (>60 years), large lesion size (>10 cm), presence of enhancing thick septa (>2 mm thick), presence of nonadipose mass-like areas, and a low proportion of fatty content (<25% of tumor volume). The signal intensity in fatty tissue within well-differentiated liposarcomas is the same as that in subcutaneous fat on T1-weighted MR images. Septa and other nonlipomatous elements show signal that is hypointense or isointense relative to that in muscle on T1-weighted MR images and hyperintense relative to that in muscle on T2-weighted MR images; these elements may enhance after the administration of contrast material (35).

## Liposarcoma

Liposarcoma is one of the most common types of soft tissue sarcoma. Malignant liposarcomas occur most frequently in the 5th and 6th decades of life, predominantly in men. Approximately 4% of liposarcomas occur in the neck; among these tumors, the most frequent sites of involvement are the neck

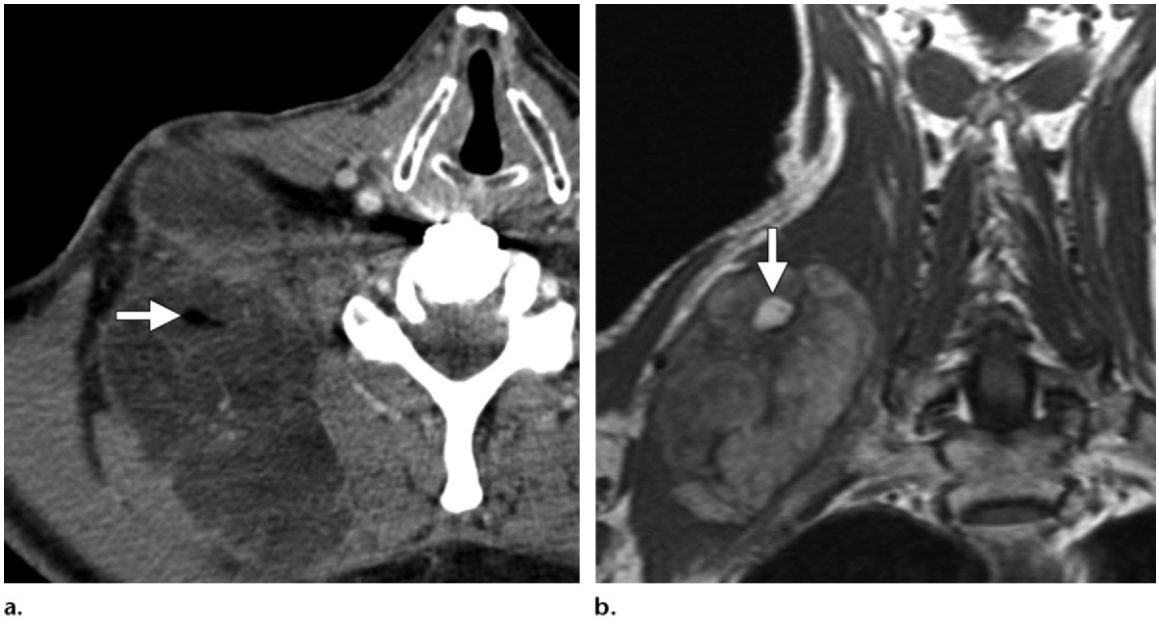

a. b.

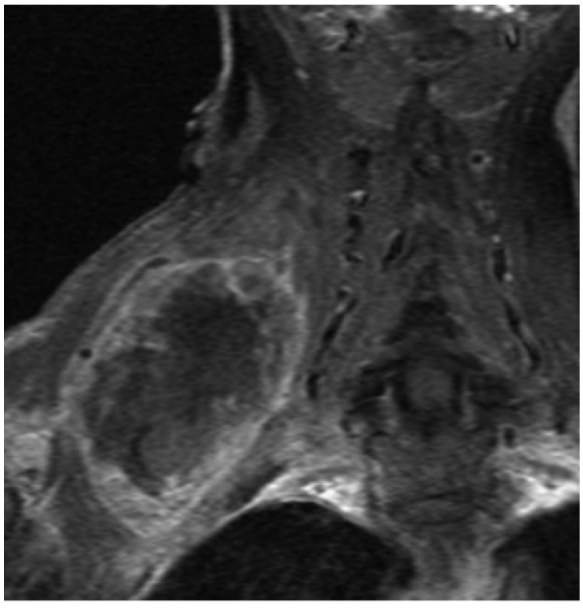

c.

**Figure 5.** Pleomorphic liposarcoma. **(a)** Axial contrast-enhanced CT scan obtained in a 59-year-old man demonstrates a right posterior cervical mass with a central focus of fat (arrow). Most of the mass shows attenuation lower than that of subcutaneous fat. **(b)** Coronal unenhanced T1-weighted MR image shows that most of the mass has signal hyperintense relative to that in muscle but hypointense relative to that in subcutaneous fat, with the exception of a small lobule in the superior portion of the tumor (arrow). Soft tissue septa are seen within the tumor. **(c)** Coronal contrast-enhanced T1-weighted fat-suppressed MR image depicts partial suppression of signal within the central portion of the mass, combined with peripheral enhancement. Although these findings are somewhat nonspecific, they should arouse the suspicion that the lesion might be a liposarcoma.

(28%), larynx (20%), and pharynx (18%). Subtypes of malignant liposarcoma include myxoid, dedifferentiated, round cell, pleomorphic, and mixed subtypes (7). The tumors vary from circumscribed lesions consisting predominantly of adipose tissue to circumscribed or infiltrating masses without any macroscopically visible adipose elements. Nonadipose components include fat necrosis and associated calcification, fibrosis, inflammation, and areas of myxoid change (2,3,5,6).

The imaging appearance of liposarcomas varies, depending on the histologic subtype. When compared with well-differentiated liposarcomas, malignant liposarcomas have a higher proportion of nonlipomatous elements; fewer than 50% of the malignant tumors contain lipid material (Fig 5). Myxoid liposarcomas may have a largely cystic appearance with nodular or diffuse enhancement. In most pleomorphic liposarcomas, adipose tissue accounts for more than 25% of the tissue volume. Adipose material, when present in liposarcomas, may be nodular, finely reticulated, or amorphous (6,35,36).

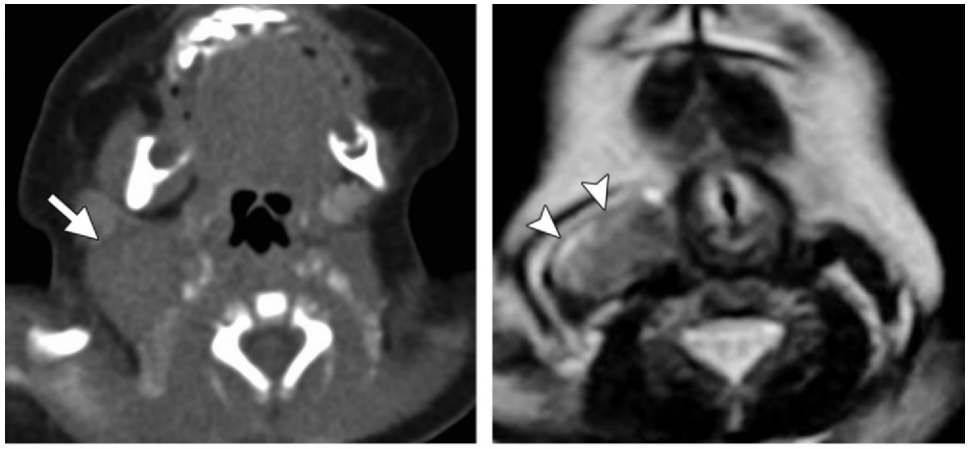

a. b.

**Figure 6.** Fibromatosis colli. **(a)** Contrast-enhanced CT scan obtained in an infant with torticollis demonstrates an enlarged right sternocleidomastoid muscle (arrow) that shows the same attenuation as other muscle. **(b)** Axial T2-weighted MR image demonstrates heterogeneously increased signal intensity in the right sternocleidomastoid muscle (arrowheads).

## Fibroblastic and Myofibroblastic Tumors

Fibroblastic and myofibroblastic tumors represent a large group of mesenchymal tumors with widely varied biologic behaviors and pathologic features. Approximately 76% of these tumors are regarded as benign, 13% as intermediate, and 11% as malignant. Roughly 27% are located in the head and neck region. These tumors represent approximately 12% of soft tissue tumors in children and adolescents, with 50% of cases diagnosed within the 1st year of life, and 71% occurring in the 1st decade (3,5).

### Fibromatosis Colli

Fibromatosis colli or sternocleidomastoid pseudotumor of infancy is a benign fibrous mass associated with torticollis in neonates and infants. It typically manifests at the age of 2–3 weeks as a firm anterior neck mass, usually on the right side, with associated torticollis. The mass typically increases in size over the course of several weeks and in 90% of cases resolves spontaneously during the next 4–8 months. The cause of fibromatosis colli is uncertain, but there is often a history of abnormal intrauterine position of the fetus or birth trauma. Pathologic evaluation demonstrates myoblasts, fibroblasts, and myofibroblasts in various stages of differentiation. US findings are usually diagnostic and include well-defined, unilateral, fusiform expansion of the sternocleidomastoid muscle. On CT scans, the sternocleiodomastoid muscle appears diffusely enlarged but shows attenuation similar to that of other muscles. At MR imaging, these pseudotumors demonstrate signal that is isointense to that of muscle on T1-weighted images and hyperintense to that of muscle on T2-weighted images, with subtle patchy and linear areas of decreased signal intensity (8) (Fig 6).

### Myofibroma

Myofibroma is the most common fibrous tumor in infants, usually manifesting before the age of 2 years. Approximately one-third of myofibromas arise in the head and neck, most commonly in the tongue, mandible, maxilla, or mastoid bone. A myofibroma is composed of contractile myoid cells arranged around thin-walled blood vessels. Boys tend to have solitary lesions (myofibroma), whereas multicentric lesions (myofibromatosis) are more common in girls. At imaging, the lesions appear round and may be well or ill defined. They usually demonstrate signal isointense to that in muscle on T1-weighted images and hyperintense to that in muscle on T2-weighted images (Fig 7), but their signal intensity varies. The center of a myofibroma may appear mildly hyperintense on T1-weighted images. Enhancement often is intense, and these lesions occasionally demonstrate a targetlike enhancement pattern (8,37).

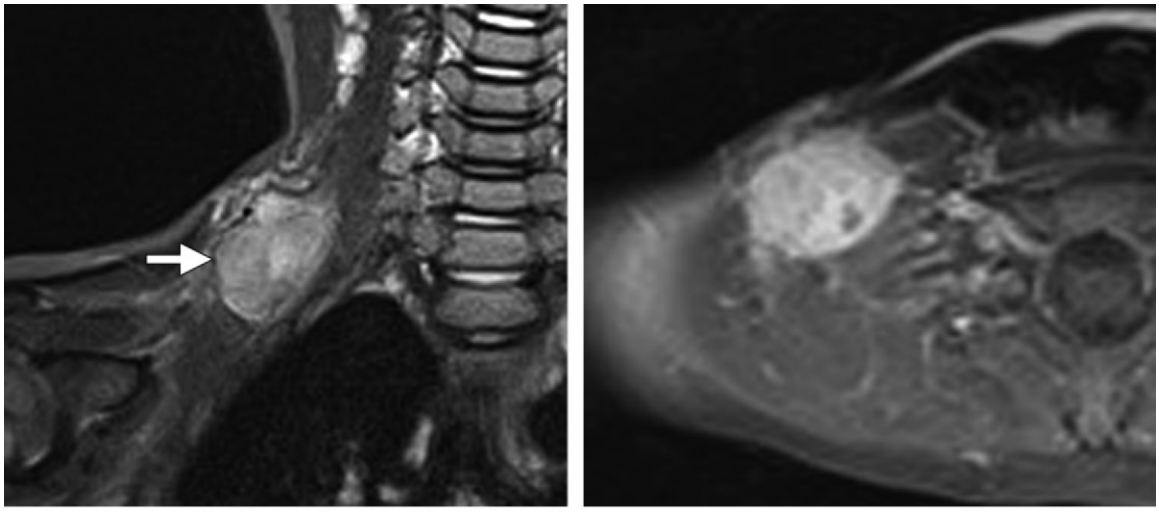

a. b.

**Figure 7.** Myofibroma. **(a)** Coronal STIR MR image obtained in a 2-year-old child demonstrates a right supraclavicular mass (arrow) abutting the scalene muscles. The mass shows signal that is hyperintense relative to that of muscle. **(b)** Contrast-enhanced T1-weighted MR image depicts marked and relatively homogeneous enhancement of the mass. These features are characteristic of myofibroma—the most common fibrous tumor in infants.

## Nodular Fasciitis

Nodular fasciitis is a mass-forming fibrous proliferation most commonly seen in the 2nd to 4th decades of life. Head and neck involvement occurs in 15%–20% of patients. The process is characterized histologically by immature fibroblasts and a variable amount of mature birefringent collagen. The pathogenesis of nodular fasciitis is unknown, and it may be a reactive or inflammatory process. Some patients report a history of trauma to the site, but most do not. Three types are described: subcutaneous, intramuscular, and intermuscular (fascial). Nodular fasciitis of the subcutaneous type occurs with a frequency three to 10 times that of other types. The intramuscular type is typically larger, deeper in location, and less well circumscribed, extending along fascial planes (38). More superficial lesions have well-defined margins, whereas deeper lesions tend to be infiltrative. The lesions vary in size from 0.5 to 10 cm.

At CT, nodular fasciitis appears as a homogeneous mass with attenuation similar to that of fluid. Associated erosion of underlying bone may be seen. At MR imaging, these tumors are heterogeneous but usually slightly hyperintense relative to muscle on T1-weighted images and hyperintense relative to muscle on T2-weighted images. Marked enhancement may be seen (39).

## Giant Cell Angiofibroma

Giant cell angiofibroma is a benign tumor that is most commonly seen in the orbital region or eyelid but also may occur in the buccal mucosa, submandibular region, or parapharyngeal space. The tumor is well circumscribed and consists of pseudovascularized spaces within a stromal matrix. Most giant cell angiofibromas occur in middle-aged adults (mean age, 45 years) (7). Orbital lesions are more common in males, whereas extraorbital lesions occur more commonly in females. The tumor may grow rapidly, simulating malignancy, or may have an indolent course with slow growth over many years. At CT, giant cell angiofibromas usually appear as circumscribed, enhancing masses. At MR imaging, they demonstrate heterogeneous signal intensity but are usually hyperintense relative to muscle on T2-weighted images and isointense relative to muscle on unenhanced T1-weighted images. Stippled areas of low signal intensity or signal void likely correspond to multiple pseudovascular spaces. Enhancement after the administration of contrast material is usually intense (Fig 8). No osseous erosion has been reported in association with a giant cell angiofibroma (40).

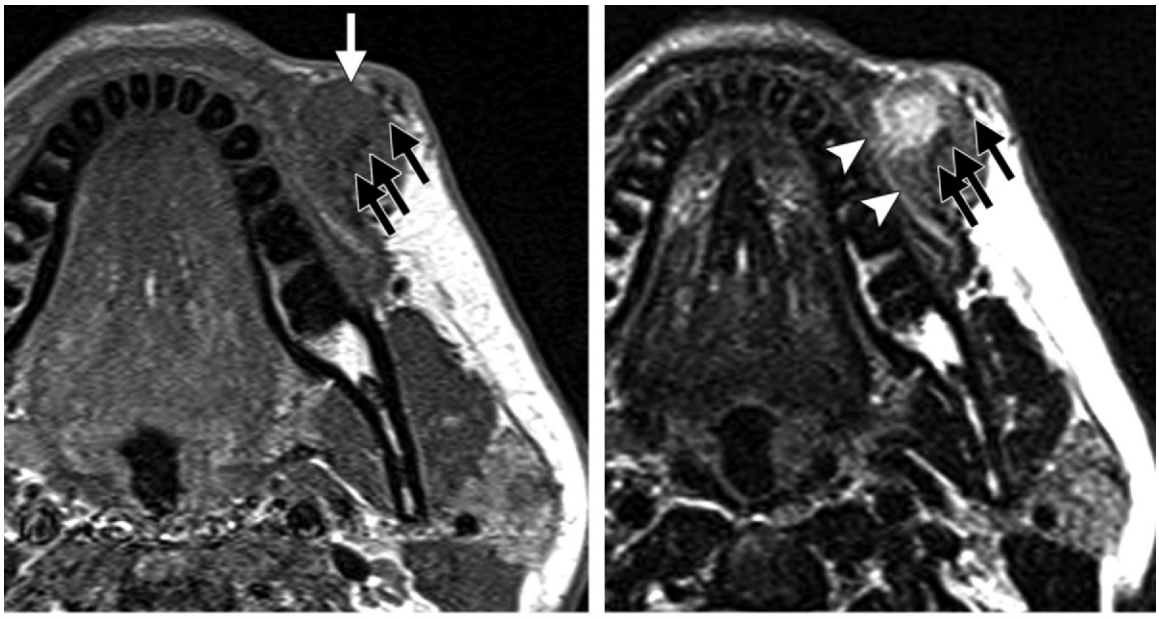

a. b.

c.

**Figure 8.** Angiofibroma. **(a)** Axial T1-weighted MR image in a 34-year-old woman shows a circumscribed, homogeneous left buccal mass (white arrow) with signal isointense to that of muscle. Black arrows = flow voids. **(b)** Axial T2-weighted MR image shows areas of high and intermediate signal intensity indicative of heterogeneous tissue components in the mass. Thickening and increased signal intensity of the underlying buccinator muscle (arrowheads) are suggestive of origin in or involvement of the muscle by the mass. Arrows = flow voids. **(c)** Contrast-enhanced T1-weighted fat-suppressed MR image depicts strong but heterogeneous enhancement within the mass. This finding, considered in conjunction with the multiple small central flow voids (arrows), is indicative of a highly vascular lesion.

## Myositis Ossificans

Myositis ossificans is a benign, self-limiting mesenchymal response to soft tissue injury. The reactive lesions are composed of hypercellular fibrous tissue, with mature bone formation usually appearing within 6–8 weeks after the onset of symptoms. The condition is most frequently seen in the 2nd and 3rd decades of life. In the head and neck, myositis ossificans has been reported in the temporalis, masseter, buccinator, and sternocleiodomastoid muscles. As the lesions mature, they shrink, and 30% of cases resolve entirely (8,41).

The imaging appearance evolves with maturation of the lesion. Initially, the MR imaging characteristics are similar to those of other soft tissue tumors and can lead to confusion. A hypointense osseous rim gradually develops and is considered diagnostic. Mature myositis ossificans lesions demonstrate the signal intensity characteristics of bone, with a well-defined, hypointense rim and trabeculae, dense fibrosis, and central adipose tissue. CT demonstrates a well-defined geometric hypodense mass with peripheral calcification in the earlier phases; mature lesions demonstrate dense calcification (8,41).

## Desmoid-Type Fibromatosis (Desmoid Tumor)

Desmoid-type fibromatosis is a locally aggressive, fibroblastic lesion with intermediate malignant potential. It is characterized by a proliferation of uni-

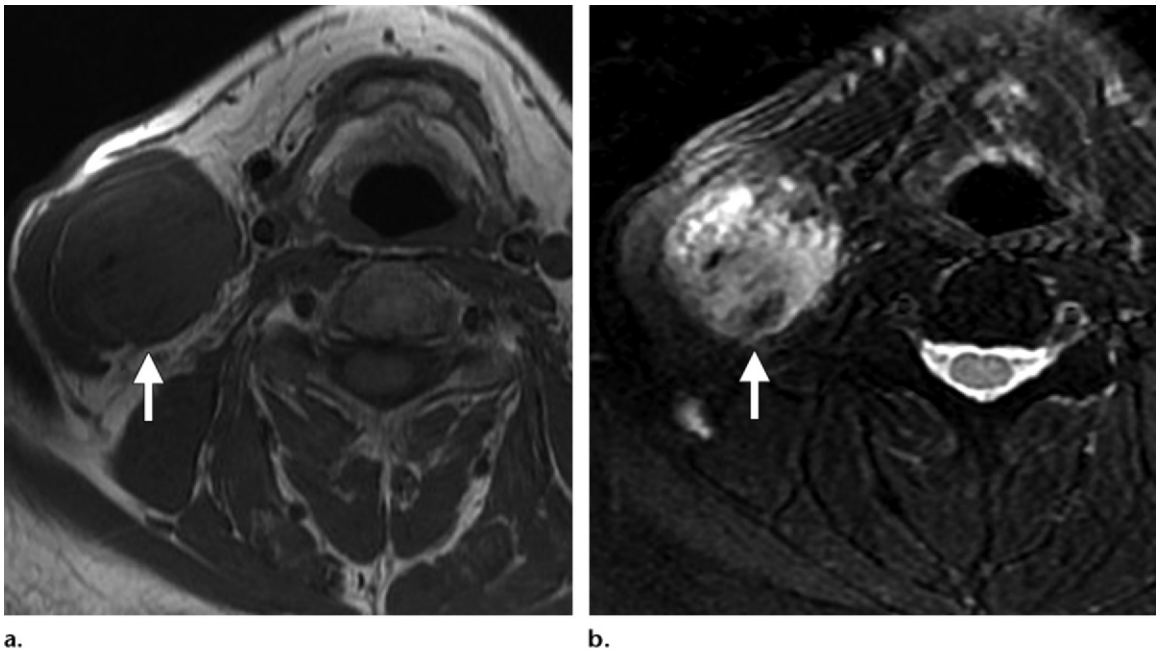

a. b.

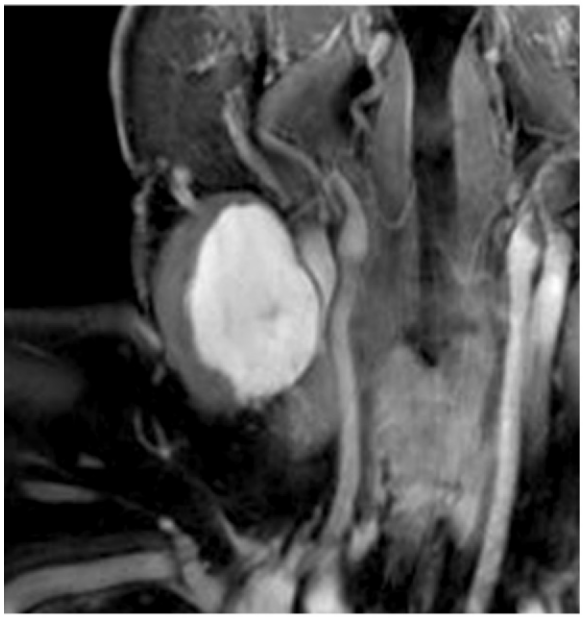

c.

**Figure 9.** Desmoid-type fibromatosis. **(a, b)** Axial T1-weighted **(a)** and T2-weighted fat-suppressed **(b)** MR images obtained in a 57-year-old man with right neck swelling demonstrate a circumscribed mass (arrow) deep to the right sternocleidomastoid muscle. The mass shows heterogeneously increased signal intensity with a few areas of diminished signal intensity on the T2-weighted image and signal isointense to that of muscle on the T1-weighted image. The mass was invading the sternocleidomastoid muscle anteriorly, as is suggested by the loss of the fat plane along the anterior margin of the tumor. **(c)** Coronal gadolinium-enhanced fat-suppressed T1-weighted image demonstrates marked homogeneous contrast enhancement within the mass, a common feature of desmoid-type fibromatosis.

form-appearing, spindle-shaped cells set in a collagenous stroma (7). It most commonly appears in the 2nd and 3rd decades of life but may be seen in people of any age. The lesion tends to behave more aggressively in children than in adults. There is often an associated history of trauma (30% of cases), and an association with Gardner syndrome also has been found (1%–2% of cases). Desmoid-type fibromatosis occurs in the head and neck in 7%–27% of cases, with the most common sites of involvement being the supraclavicular and neck regions, followed by the face. The lesion is typically poorly circumscribed, with infiltration of the surrounding soft tissues and, often, fixation to underlying muscle or bone. There is a 70% rate of recurrence after resection (2,5,6).

The MR imaging appearance of desmoid-type fibromatosis varies, depending in part on the cellularity of the lesion and the amount of collagen and myxoid material within it. Signal within the mass is typically isointense or slightly hyperintense on T1-weighted images and isointense or heterogeneously hyperintense on T2-weighted images relative to signal intensity in muscle. Linear and curvilinear strands with decreased signal intensity on T1-weighted and T2-weighted images may represent collagen fibers within a desmoid tumor, and if such features are extensive, they are suggestive of the diagnosis. Intense enhancement is a common feature of these tumors (42) (Fig 9).

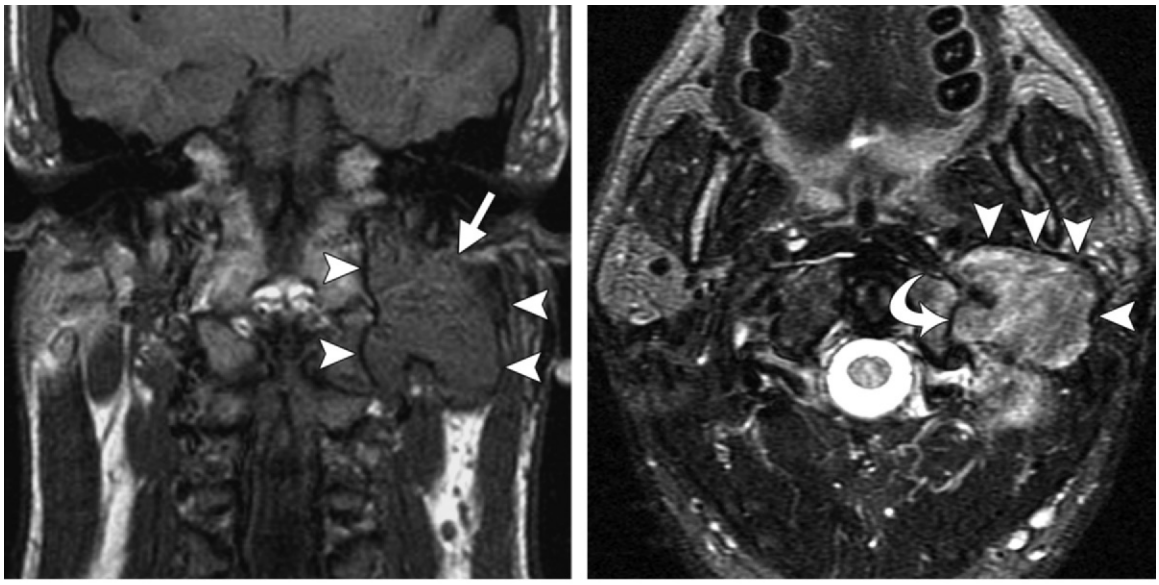

a. b.

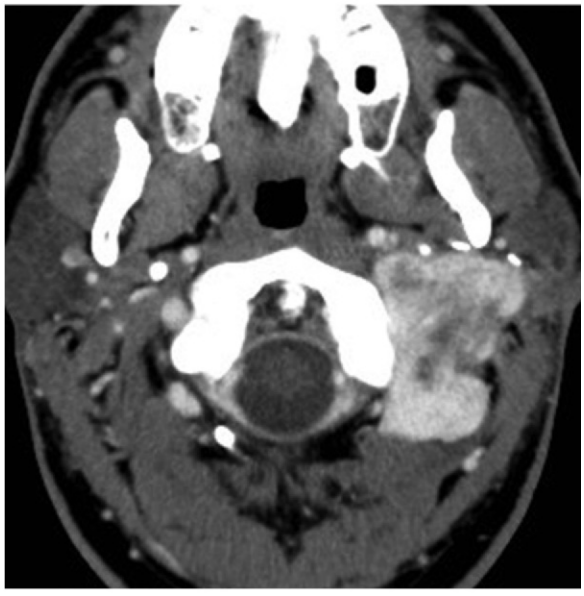

c.

**Figure 10.** Recurrent hemangiopericytoma. **(a)** Coronal unenhanced T1-weighted image obtained in a 33-year-old man who had undergone previous tumor resection demonstrates a circumscribed, homogeneous, left paraspinal mass (arrow) with signal that is slightly hyperintense relative to that in muscle. Arrowheads = pseudocapsule. **(b)** Axial T2-weighted MR image shows heterogeneous, predominantly hyperintense signal in the mass relative to signal intensity in muscle. The mass extends into the transverse foramen (arrow) at this level. Note the peripheral rim of low signal intensity (arrowheads), which presumably represents a pseudocapsule. **(c)** Contrast-enhanced CT image demonstrates avid tumor enhancement, a frequent feature of hemangiopericytomas.

## Solitary Fibrous Tumor and Hemangiopericytoma

Solitary fibrous tumor and hemangiopericytoma are rarely metastasizing tumors with intermediate malignant potential. The distinction between these two tumor types has become increasingly blurred because their histopathologic features largely overlap; as a result, there is controversy about the use of the terms. Some experts believe that the majority of lesions previously referred to as hemangiopericytomas are in fact solitary fibrous tumors. Currently accepted histopathologic categories, along with the WHO system for classifying soft tissue tumors, acknowledge these changes by classifying most hemangiopericytomas as solitary fibrous tumors (7). Typical solitary fibrous tumors have a patternless architecture characterized by alternating hypocellular and hypercellular areas separated by thick bands of hyalinized collagen and branching vessels. Hemangiopericytomas closely resemble the cellular areas of solitary fibrous tumors and show clinical behavior similar to that of solitary fibrous tumors. Both tumors usually occur in middle-aged adults, typically manifesting as slow-growing, painless masses. They may be locally infiltrative, and they are occasionally associated with systemic symptoms such as hypoglycemia (because of overproduction of an insulinlike growth factor), arthralgia, and osteoarthropathy, as well as digital clubbing.

Most solitary fibrous tumors of the head and neck arise in the nasal cavity or paranasal sinuses. They are also found in the nasopharynx, parapharyngeal space, and larynx. Hemangiopericyto-

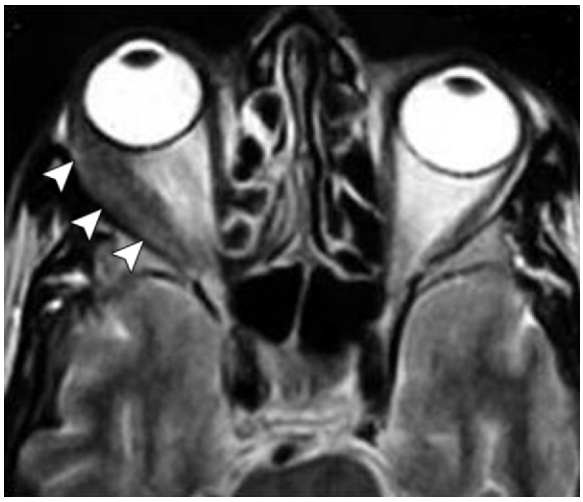

**Figure 11.** Orbital inflammatory myofibroblastic tumor (pseudotumor). Axial T2-weighted MR image demonstrates right proptosis and enlargement of the right lateral rectus muscle (arrowheads), which appears hypointense relative to gray matter. Signal hypointensity in the lesion on T2-weighted MR images is suggestive of orbital pseudotumor but is an insensitive diagnostic sign. The retrobulbar fat on the right shows higher signal intensity than normal, a finding suggestive of early infiltration by a pseudotumor.

mas most commonly arise in the pelvic retroperitoneum and limbs and are less likely than solitary fibrous tumors to occur in the head and neck. Both tumors can also arise intracranially from the meninges. At MR imaging, these tumors appear as well-circumscribed, solid masses with low to intermediate signal intensity on T1-weighted images and heterogeneously high signal intensity on T2-weighted images. T2-weighted images may also show a low-signal-intensity rim representing a pseudocapsule around the lesion (43) (Fig 10). The tumors demonstrate variable enhancement, but enhancement is often intense because of their high vascularity (44,45).

## Inflammatory Myofibroblastic Tumor (Inflammatory Pseudotumor)

Inflammatory myofibroblastic tumor, also commonly referred to as inflammatory pseudotumor, most frequently occurs in middle-aged people and shows no predilection for either sex. It is commonly seen in the orbit but may also occur in the thyroid gland and at the skull base. It is associated with fibrosing mediastinitis and retroperitoneal fibrosis. The tumors have intermediate malignant potential but rarely metastasize. They are composed of myofibroblastic spindle cells with an inflammatory infiltrate of plasma cells, lymphocytes, and eosinophils (7,46).

Inflammatory pseudotumor is the third most common primary tumor of the orbit and a common cause of unilateral proptosis in adults. It constitutes about 6% of all orbital lesions and is usually unilateral. Patients classically present with an acute onset of eye pain associated with ophthalmoplegia, decreased vision, or proptosis. Uveal and scleral thickening is seen in 33% of patients with orbital pseudotumor and is thought to be a specific sign (47). Bone destruction and intracranial extension of orbital pseudotumor are rare but have been reported (46–48).

Several subcategories of orbital inflammatory pseudotumors are distinguished on the basis of the anatomic structures involved in the inflammatory process, but these subcategories often coexist in a single case. The myositis-related form, which is the most common, affects the extraocular muscles; the dacryoadenitis-related form affects the lacrimal glands; the neuritis-associated form affects the optic nerve sheath; the apical form affects the structures of the orbital apex; the episcleral form affects the anterior orbit, including the sclera and preseptal soft tissues; and, finally, the diffuse form affects the entire orbit (49).

Extraorbital inflammatory pseudotumors of the head and neck occur most frequently in the nasal cavity, followed by the nasopharynx, skull base, temporal bone, maxillary sinus, larynx, trachea, thyroid gland, and salivary glands. Perineural spread along maxillary, mandibular, and hypoglossal nerves, and internal carotid occlusion, can occur. Sinonasal pseudotumors usually have a more aggressive appearance than orbital pseudotumors because they commonly produce osseous erosion, remodeling, and sclerosis. Extraorbital pseudotumors are less responsive to steroid therapy than orbital pseudotumors, but the prognosis after complete resection is good (46).

At imaging, inflammatory pseudotumors may appear circumscribed or poorly defined with extensive surrounding inflammatory changes. The CT characteristics of inflammatory pseudotumors are nonspecific, with both attenuation and enhancement varying. At MR imaging, inflammatory pseudotumors usually show signal that is isointense or hypointense relative to that in muscle on T1-weighted images, and variable relative to that in muscle on T2-weighted images. In some cases, the pseudotumors may appear hypointense on T2-weighted images (Fig 11). Variable contrast enhancement can be seen (46).

### Fibrosarcoma

Fibrosarcoma is a malignant tumor of fibroblasts demonstrating a classic herringbone-like architecture. The tumor accounts for 1%–3% of sarcomas in adults and 11%–12% of sarcomas in infants. Most adult fibrosarcomas occur in patients between the ages of 40 and 70 years, with a pronounced male predominance (60%). Infantile fibrosarcoma is histologically identical to classic adult fibrosarcoma but is associated with a much better prognosis. Most cases of infantile fibrosarcoma occur before 2 years of age (50). As mentioned earlier, fibrosarcomas may be associated with previous irradiation of the head and neck.

Patients present with an enlarging mass, which may be painful or painless. In the head and neck region, fibrosarcoma may arise in the sinonasal cavities, larynx, or neck. Storiform-pleomorphic (50%–60%), myxoid (25%), giant cell (5%–10%), and inflammatory (5%) subtypes of fibrosarcoma are distinguished. At MR imaging, the tumors have nonspecific features, typically demonstrating heterogeneous, predominantly low signal intensity with variable enhancement on T1-weighted images and heterogeneous high signal intensity on T2-weighted images (2,3,5,6) (Fig 12).

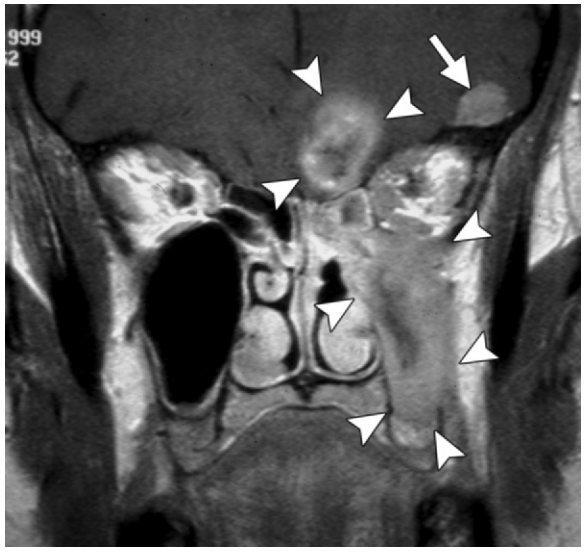

**Figure 12.** Fibrosarcoma. Coronal contrast-enhanced T1-weighted MR image obtained in a 36-year-old patient who had undergone head and neck irradiation for retinoblastoma in early childhood demonstrates a moderately enhancing partially necrotic mass (arrowheads) that involves the left maxillary and ethmoid sinuses and extends through the anterior skull base into the anterior cranial fossa. Note the erosion of the left lateral maxillary sinus wall and left orbital floor. A meningioma (arrow) in the floor of the left anterior cranial fossa is probably also radiation induced.

## So-called Fibrohistiocytic Tumors

The classification of this group of tumors has been in flux since it became evident that the majority are not truly histiocytic. The traditional category of so-called fibrohistiocytic tumors includes benign lesions such as pigmented villonodular synovitis and deep benign fibrous histiocytoma, intermediate lesions such as giant cell tumor of the soft tissues, and malignant lesions such as malignant fibrous histiocytoma (7). Although malignant fibrous histiocytoma has been reclassified as an undifferentiated form of sarcoma, many observers continue to use the term *malignant fibrous histiocytoma*, either out of habit or because of the complexity of the new terminology (4).

### Deep Benign Fibrous Histiocytoma

Benign fibrous histiocytoma is a tumor composed of a biphasic cell population of histiocytes and fibroblasts arising either from the skin (cutaneous benign fibrous histiocytomas) or subcutaneous soft tissues (deep benign fibrous histiocytomas). The cutaneous form does not usually require imaging evaluation. Deep benign fibrous histiocytomas are rare, accounting for less than 1% of histiocytic tumors. They are usually found in adults older than 25 years, predominantly men (7). In the head and neck, the tumors most commonly occur in subcutaneous tissues or in the orbit. They may also arise from the mandible, maxilla, or pterygopalatine fossa. Malignant transformation occurs in approximately 1% of deep benign fibrous histiocytomas (51). Unfortunately, benign fibrous histiocytomas have a nonspecific imaging appearance and cannot be reliably differentiated from malignant fibrous histiocytomas at either CT or MR imaging (see the section on "Malignant Fibrous Histiocytoma [Undifferentiated Pleomorphic Sarcoma]") (52).

### Diffuse-Type Giant Cell Tumor (Pigmented Villonodular Synovitis)

Diffuse-type giant cell tumor, also commonly referred to as pigmented villonodular synovitis, is a benign but locally destructive proliferation of mononuclear cells that resemble those in the synovium, admixed with multinuclear giant cells and inflammatory cells. This tumor typically

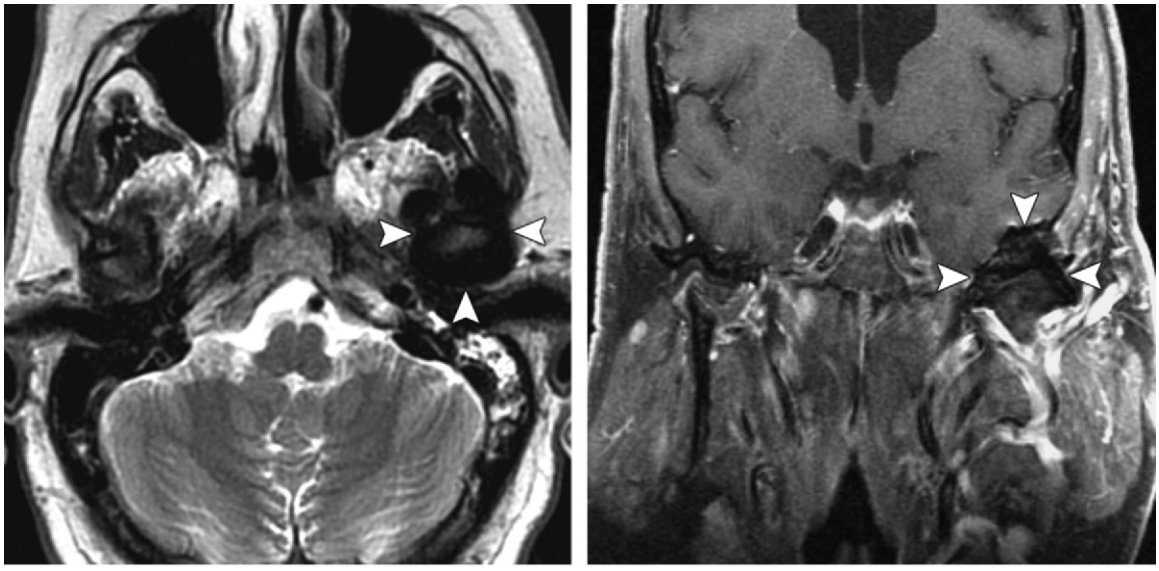

a. b.

**Figure 13.** Pigmented villonodular synovitis. Axial T2-weighted **(a)** and coronal contrast-enhanced T1-weighted fat-suppressed **(b)** MR images obtained in a 53-year-old man with a left ear mass and progressively changing bite demonstrate a markedly hypointense mass (arrowheads) that has enveloped the left mandibular condyle, a characteristic appearance of pigmented villonodular synovitis. Only slight enhancement is evident on the T1-weighted image.

affects tendon sheaths or joints, most often in adults younger than 40 years. In the head and neck, pigmented villonodular synovitis frequently arises in the temporomandibular joint. This lesion has a predilection to hemorrhage, resulting in hemosiderin deposition. As a result, the tumor characteristically appears as an aggressive mass that partially encases the mandibular condyle and demonstrates low signal intensity on both T1- and T2-weighted MR images (Fig 13). The tumor typically erodes the adjacent skull base and mandibular ramus and may extend into the middle cranial fossa. Mild or peripheral enhancement is seen within the tumor after contrast material administration (53).

## Malignant Fibrous Histiocytoma (Undifferentiated Pleomorphic Sarcoma)

Malignant fibrous histiocytoma was previously thought to be the most common type of adult sarcoma (20%–30%); however, many tumors that previously would have been classified as malignant fibrous histiocytomas are no longer grouped in that category. The category itself has been renamed *undifferentiated pleomorphic sarcoma,* a term that more accurately conveys the histologic content of the tumors, which can be diagnosed only by a process of exclusion. It is now estimated that malignant fibrous histiocytomas actually account for roughly 5% of adult sarcomas. Only 3%–10% of undifferentiated pleomorphic sarcomas occur in the head and neck region. The peak incidence is among people in the 6th to 7th decade of life, predominantly males (70%). In the head and neck, the tumors are most commonly located in the sinonasal region (46%), the soft tissue of the face and neck (38%), the oral cavity (8%), or the craniofacial bones (8%). Several morphologic subtypes are described, including storiform-pleomorphic (50%–60%), myxoid (25%), giant cell (5%–10%), and inflammatory (5%), although more than one of these morphologic patterns may be observed in a lesion. The myxoid variant is associated with a better prognosis, compared with the storiform-pleomorphic type. The tumor has a local recurrence rate ranging from 19% to 31% and a rate of metastasis estimated at 31%–35%. Common sites of metastasis are the lungs (90%), bones (8%), and liver (1%). The incidence of regional lymph node metastasis is 4%–17% (3,54). Like fibrosarcoma, undifferentiated pleomorphic sarcoma is associated with previous irradiation.

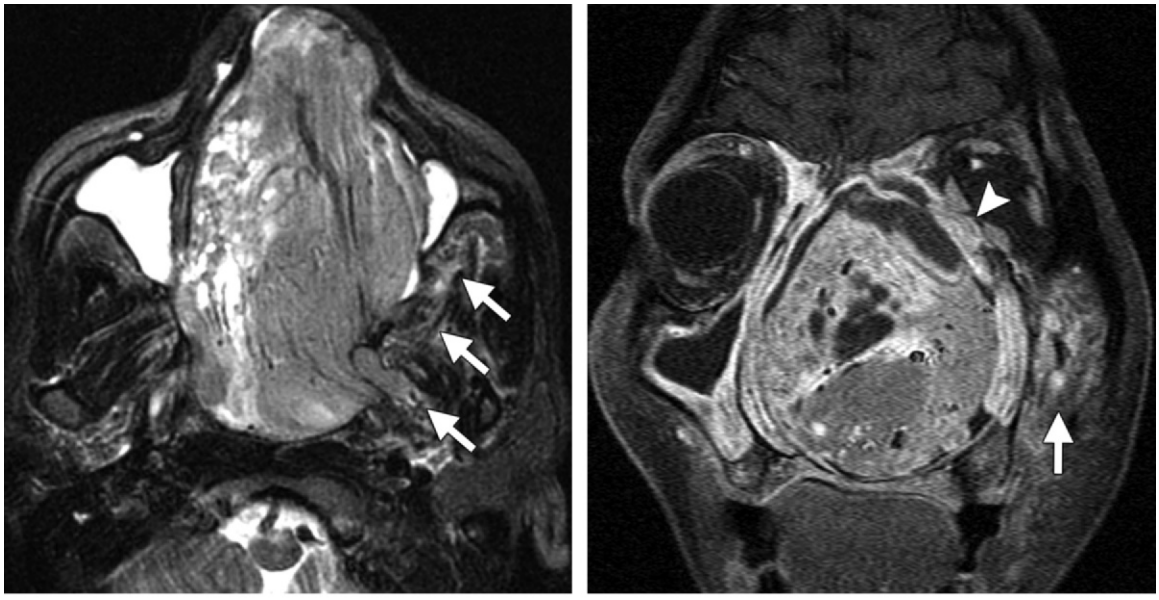

a. b.

**Figure 14.** Malignant fibrous histiocystoma. **(a)** Axial T2-weighted MR image obtained in a 53-year-old man shows a large, expansile mass that fills the nasal cavity and nasopharynx, obliterating all the normal sinonasal structures and infiltrating the left masticator space (arrows). The mass has a heterogeneous appearance with signal that is mildly hyperintense relative to that in muscle. **(b)** Coronal contrast-enhanced fat-suppressed T1-weighted MR image demonstrates heterogeneous enhancement of the tumor, which has infiltrated the infratemporal fossa (arrow) and left orbit (arrowhead). Nonenhancing cystic regions within the tumor probably represent myxomatous elements, necrosis, or both. The large size and heterogeneous appearance of the tumor, its destruction of bone, and its extracompartmental extension are highly suggestive of malignancy.

The CT and MR imaging features of the tumors are nonspecific. At CT, undifferentiated pleomorphic sarcoma appears as a large, lobulated soft tissue mass with attenuation similar to that of muscle. Calcification or ossification can be observed in 5%–20% of the tumors. The center of the tumor often shows diminished attenuation because of necrosis, hemorrhage, or myxoid material. At MR imaging, the tumors typically have signal intensity similar to that of muscle on T1-weighted images and heterogeneously hyperintense relative to that of muscle on T2-weighted images; variable enhancement is seen in the solid portions of the tumors. Myxoid tumor regions may show signal intensity similar to that of fluid on T1- and T2-weighted images, with nodular and peripheral enhancement of nonmyxomatous cellular regions (54,55) (Fig 14).

## Skeletal Muscle Tumors

The WHO classification of skeletal muscle tumors includes variants of two general entities: rhabdomyoma and rhabdomyosarcoma (7).

### Rhabdomyoma

Rhabdomyomas occur in two forms: a common cardiac form, and a rare extracardiac form. Extracardiac rhabdomyomas are benign tumors consisting of immature striated muscle cells, and between 70% and 90% of these tumors are found in the head and neck. There are two subtypes: adult and fetal. Adult rhabdomyomas predominantly affect men in the 5th decade of life and are most often found in the larynx, pharynx, or oral cavity. Because of their slow rate of growth, adult rhabdomyomas often become large. Fetal rhabdomyomas, which are composed of immature skeletal muscle cells, are primarily found in males at a median age of 4 years. They are located in subcutaneous tissue, with a particular predilection for the postauricular region (7).

The appearance of rhabdomyomas at both CT and MR imaging is nonspecific. These tumors generally demonstrate signal intensity similar to that in muscle on T1- and T2-weighted MR images and usually enhance after the administration of contrast material at both MR imaging and CT (6,56).

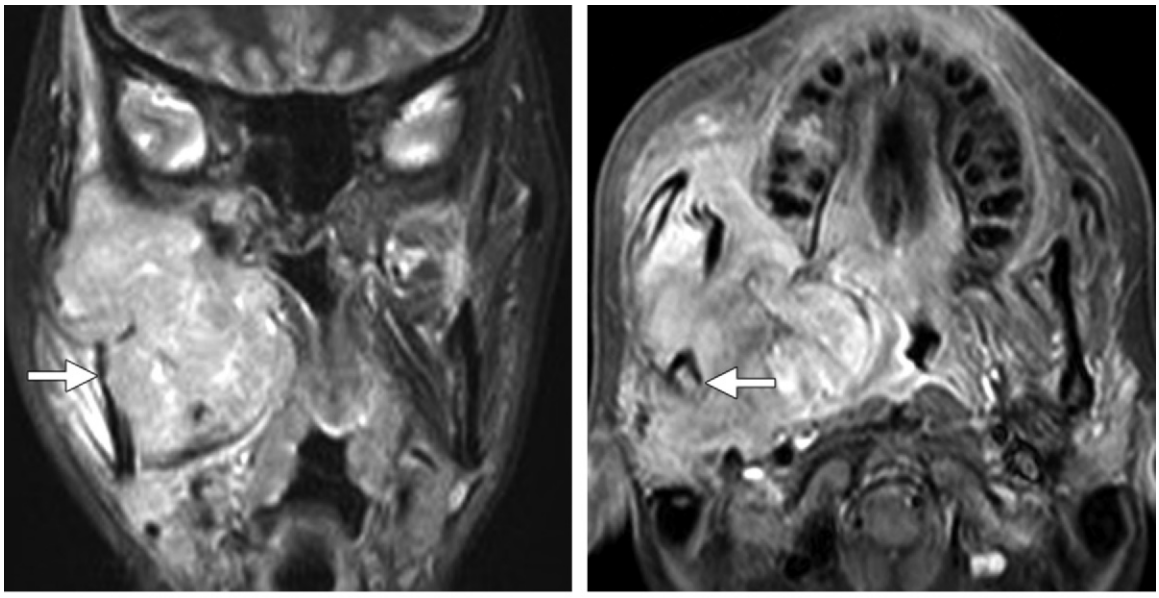

a. b.

**Figure 15.** Rhabdomyosarcoma. **(a)** Coronal T2-weighted MR image obtained in a 31-year-old woman demonstrates a large, aggressive, heterogeneously hyperintense mass (arrow) that is centered in the right masticator space and displaces the nasopharyngeal airway leftward. **(b)** Axial contrast-enhanced T1-weighted fat-suppressed image shows avid enhancement of the mass, which has eroded and invaded the adjacent mandible (arrow).

## Rhabdomyosarcoma

Rhabdomyosarcoma, which arises from primitive undifferentiated mesenchymal cells, is the most common soft tissue sarcoma in children but also affects adults (12). The disease has a bimodal distribution, with one peak occurring during the 1st decade of life and the second occurring during adolescence. Three subtypes of rhabdomyosarcoma are recognized: The embryonal subtype (70%), which includes the botryoid subtype, affects young children and is associated with a relatively good prognosis. The alveolar subtype (15%), which is seen in older children, is associated with a worse prognosis. The rare, pleomorphic subtype of rhabdomyosarcoma contains variable amounts of hemorrhage and necrosis and is usually seen in adults; this subtype also implies a poor prognosis (8,12).

Approximately 40% of cases of rhabdomyosarcoma occur in the head and neck, in sites that are categorized as parameningeal (50%), nonparameningeal (25%), or orbital (25%). Parameningeal lesions arise in sites with a close anatomic relationship to the meninges, including the nasopharynx and nasal cavity, middle ear and mastoid, paranasal sinuses, and pterygopalatine and infratemporal fossae; these generally are associated with a worse prognosis than tumors arising in other sites (57). Rhabdomyosarcomas are typically aggressive tumors that erode bone. Metastatic cervical adenopathy is seen in approximately 10%–20% of cases, and distant metastases are seen in approximately 15% of cases at the time of presentation (8,12,58).

At imaging, rhabdomyosarcomas appear as relatively well circumscribed soft tissue tumors that are often accompanied by lytic bone destruction. On contrast-enhanced CT or MR images, variable tumor enhancement is observed (Fig 15). The signal intensity of tumors on T2-weighted MR images also is variable; occasionally, highly cellular rhabdomyosarcomas may appear iso- to hypointense relative to the brain. Coronal contrast-enhanced T1-weighted MR imaging is especially useful for detecting parameningeal tumors. The embryonal subtype of rhabdomyosarcoma may demonstrate hemorrhage, necrosis, and calcification, features that produce a more heterogeneous enhancement pattern. The botryoid subtype of embryonal rhabdomyosarcoma may show multiple ringlike enhancing features that resemble a bunch of grapes. In some tumors of the alveolar subtype, serpentine flow voids may be seen (58,59).

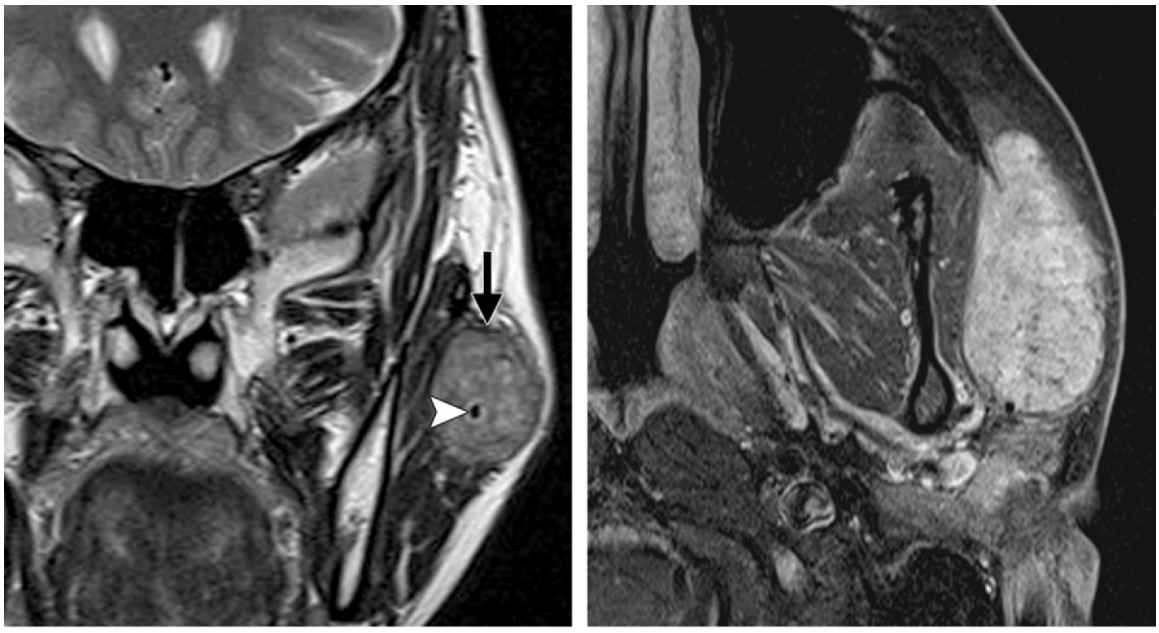

a. b.

**Figure 16.** Angioleiomyoma. **(a)** Coronal T2-weighted MR image obtained in a 45-year-old woman demonstrates a well-circumscribed, heterogeneously hyperintense mass (arrow) arising from the left masticator space, just superficial to the masseter muscle. Note the prominent flow void (arrowhead) near the center of the mass. **(b)** Axial contrast-enhanced T1-weighted fat-suppressed MR image shows avid enhancement of the mass.

## Smooth Muscle Tumors

In the WHO system of classification, the category of smooth muscle tumors includes leiomyoma, angioleiomyoma, and leiomyosarcoma. Noncutaneous, nonuterine leiomyomas of deep soft tissue are exceedingly rare and occur primarily in the extremities and abdomen (7). For these reasons, they are not discussed in detail here.

### Angioleiomyoma

Angioleiomyomas, or vascular leiomyomas, are relatively common benign tumors composed of mature smooth muscle bundles surrounding vascular channels. They occur predominantly in women in the 3rd through 6th decades of life. These tumors manifest as slow-growing, firm, sometimes painful masses (60). Approximately 8.5% of angioleiomyomas are found in the head and neck region, with sites of occurrence including the oral cavity, lip, auricle, submandibular region, sinonasal cavities, buccal space, larynx, and masticator space (61,62).

CT demonstrates a well-defined mass containing numerous blood vessels. At MR imaging, angioleiomyomas appear internally heterogeneous, with intermediate to low signal intensity on T1-weighted images and intermediate to high signal intensity on T2-weighted images. The tumors enhance, often avidly, after the administration of contrast material, and flow voids are frequently evident (3,60) (Fig 16).

### Leiomyosarcoma

Leiomyosarcoma is a high-grade malignancy that accounts for approximately 6% of all soft tissue sarcomas (63). It is believed to originate most frequently from smooth muscle cells within the walls of blood vessels, but it may also arise from undifferentiated mesenchymal cells. The mean age at diagnosis is 50 years. Between 3% and 10% of leiomyosarcomas occur in the head and neck, primarily in the nasal cavity and paranasal sinuses. Other sites include the skin, cervical esophagus, and larynx. Trauma, irradiation, chemotherapy, human immunodeficiency virus (HIV) infection, a history of retinoblastoma, and sunlight exposure have been described as possible contributing factors (5,6,64).

The imaging features of leiomyosarcomas are nonspecific. At CT, they typically appear as bulky masses that remodel bone and show little enhancement. Calcification is uncommon. At MR imaging, they typically show signal that is iso- to hypointense relative to that in muscle on T1-weighted images and variably hyperintense relative to that in muscle on T2-weighted images, with prominent contrast enhancement. Large lesions are usually more heterogeneous in

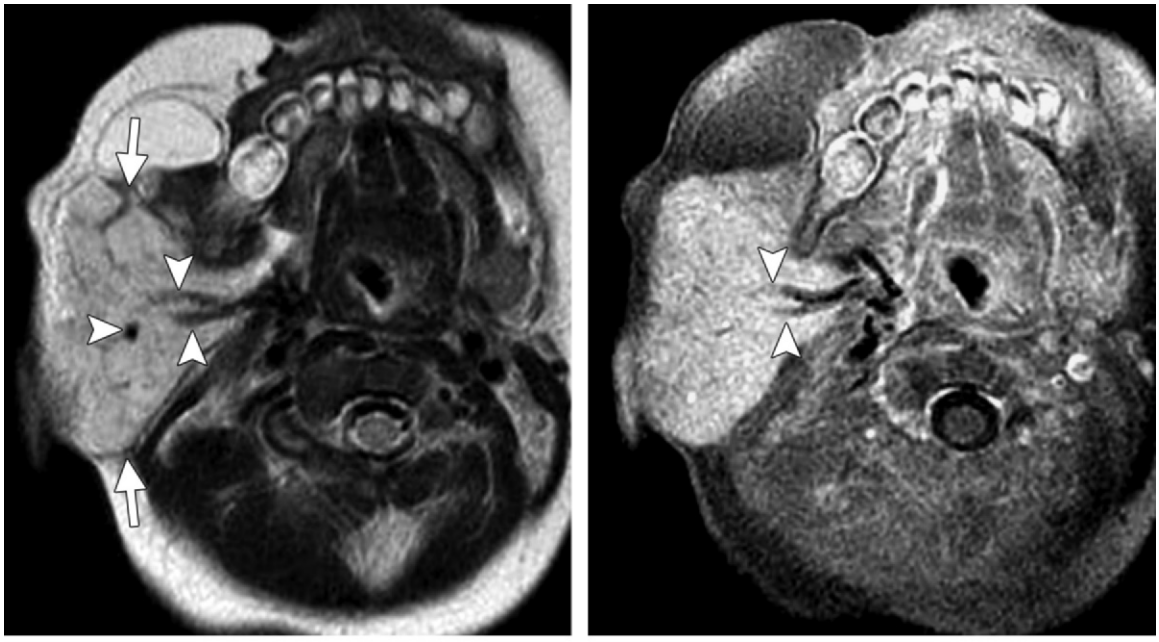

a. b.

**Figure 17.** Infantile hemangioma in an 8-week-old girl with an enlarging mass in her right cheek. **(a)** Axial T2-weighted MR image demonstrates a homogeneously hyperintense, multicompartmental mass (arrows) in the right parotid, parapharyngeal, and buccal spaces, with several branching flow voids (arrowheads). The mass exhibits signal only slightly less intense than that in adjacent fat. **(b)** Axial contrast-enhanced T1-weighted fat-suppressed MR image shows intense homogeneous enhancement of the mass. Arrowheads = flow voids.

appearance, with regions of hemorrhage, necrosis, and cystic change (4,63,65).

## Vascular Tumors

The category of vascular tumors includes benign entities such as hemangioma and lymphangioma, intermediate entities such as kaposiform hemangioendothelioma and Kaposi sarcoma, and malignancies such as epithelioid hemangioendothelioma and angiosarcoma (7).

### Hemangioma

Because it is often difficult to determine histologically whether a benign vascular tumor is a malformation or a neoplasm, a wide variety of vascular lesions may be classified as hemangiomas in the WHO system. A more helpful clinical classification system may be that proposed by Mulliken and colleagues, which divides vascular anomalies into vascular tumors (hemangiomas) and vascular malformations (eg, capillary, lymphatic, venous, arteriovenous) (66,67). A review of all of these lesions is beyond the scope of the article, and they are well described elsewhere (68). Therefore, we have limited our discussion of hemangiomas to the extremely common infantile hemangioma.

Infantile hemangiomas are the most common vascular tumors and occur primarily in the head and neck region. They are more common in girls than in boys. They typically appear in early infancy, rapidly enlarge during the 1st year of life, and thereafter slowly involute over the course of several years. During the growth phase, hemangiomas display prominent vascularity, whereas the involution phase is characterized by decreasing vascularity and shrinkage of the mass, accompanied by an increase in fibrofatty tissue content. Approximately 20% of children affected have multiple hemangiomas (68–71).

Proliferating hemangiomas are well circumscribed but often transspatial. They show attenuation similar to that of muscle on unenhanced CT images and enhance rapidly and intensely after the intravenous administration of a contrast agent. At MR imaging, prominent vascularity appears as conspicuous flow voids on SE images and as flow-related enhancement on gradient-echo images. Proliferating hemangiomas appear moderately to markedly hyperintense on T2-weighted MR images and enhance intensely (Fig 17). Involuting hemangiomas progressively shrink and demonstrate an increasing fibrofatty matrix, reduction in vascularity, and a relative decrease in enhancement. The imaging features, in conjunction with the age of the child, usually permit a specific diagnosis (68–71).

### Kaposiform Hemangioendothelioma

Kaposiform hemangioendothelioma is a locally aggressive vascular tumor of infancy that is distinguished pathologically from the more common hemangioma of infancy on the basis of its infiltrative growth pattern and predominant Kaposi sarcoma–like content consisting of fascicles of spindle cells. The tumors also may demonstrate fibrinogenic thrombi in the capillaries, hemorrhage, and foci resembling lymphangiomatosis, with the last finding being described in about two-thirds of cases (7). Most of these tumors are manifested within the 1st year of life, and roughly half of them are present at birth. The most relevant associated clinical condition is consumptive coagulopathy (Kasabach-Merritt syndrome), which occurs in more than 50% of cases (10).

In comparison with infantile hemangiomas, kaposiform hemangioendotheliomas are more likely to demonstrate ill-defined margins; involvement of multiple tissue planes, with cutaneous thickening, stranding of subcutaneous fat, hemorrhage, and destructive changes; and remodeling of adjacent bone. They also may encase the cervical vessels (72). At MR imaging, kaposiform hemangioendotheliomas demonstrate signal intensity similar to that of muscle on T1-weighted images and heterogeneously hyperintense relative to that of muscle on T2-weighted images, with apparent infiltration of the subcutaneous tissues. Signal voids representing accumulations of blood products may be evident on gradient-echo MR images. Diffuse heterogeneous enhancement is usually seen after the administration of contrast material (10,68,72,73).

### Kaposi Sarcoma

Kaposi sarcoma is a multicentric malignant vascular tumor of unknown etiology arising from endothelial cells. Four clinical patterns have been described: classic, Africa-endemic, acquired immunodeficiency syndrome (AIDS)-related, and iatrogenic; the last pattern is seen in transplant recipients and others who undergo immunosuppressive therapy. Most occurrences of Kaposi sarcoma in the head and neck are AIDS related, and all forms of Kaposi sarcoma are associated with herpesvirus 8 infection. Cutaneous involvement is seen in 66% of those affected, mucosal disease (intraoral, pharyngeal, laryngeal, and nasal cavity) is present in 56%, and nodal involvement is seen in 13% (74). At CT, Kaposi sarcoma manifests as multiple nodular cutaneous or mucosal lesions, which characteristically enhance avidly (Fig 18). At MR imaging, the appearance of the lesions is nonspecific, with low signal intensity on T1-weighted images, high signal intensity on T2-weighted images, and usually strong contrast enhancement (5,74,75).

### Soft Tissue Angiosarcoma

Angiosarcoma is an aggressive vascular malignancy with high rates of local recurrence and distant metastasis. Soft tissue angiosarcoma may occur in people of any age but is more common in older patients, with a peak incidence in the 7th decade of life. Independent risk factors for angiosarcoma include chronic lymphedema, previous radiation therapy, and familial syndromes including type 1 neurofibromatosis, Klippel-Trénaunay-Weber syndrome, and Maffucci syndrome. These tumors are also associated with foreign bodies and immunosuppression (7,76).

The MR signal characteristics of angiosarcoma include intermediate signal intensity on T1-weighted images and high signal intensity on T2-weighted images. Aggressive infiltration of adjacent tissues is seen. Areas of high signal intensity representing hemorrhage may be seen on T1-weighted images. The signal intensity of vascular structures within the tumors may reflect high flow (low signal intensity on all MR images regardless of pulse sequences) or low flow (high signal intensity on T2-weighted images). The tumors enhance after the administration of intravenous gadolinium-based contrast material and may demonstrate central areas of necrosis (4,77).

## Pericytic Tumors: Sinonasal Glomus Tumor

Pericytic tumors show differentiation toward myoid-contractile perivascular cells and a characteristic tendency to grow in a circumferential perivascular pattern. True pericytic tumors in-

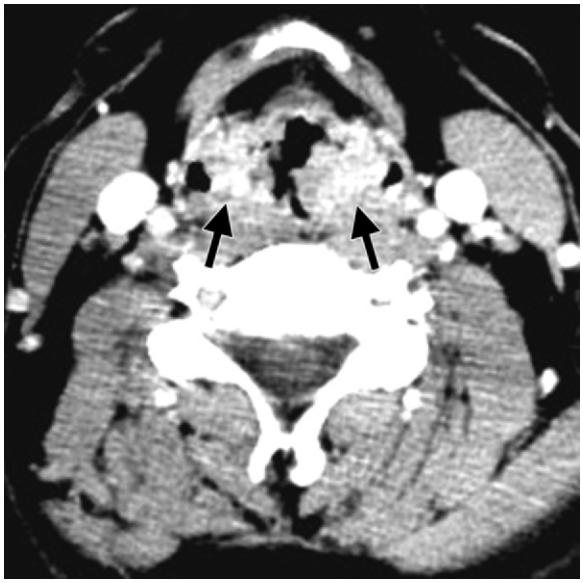

**Figure 18.** Kaposi sarcoma in a 35-year-old man. Axial contrast-enhanced CT scan obtained at the level of the supraglottic larynx demonstrates nodular thickening and marked enhancement of the aryepiglottic folds (arrows). There was no lymphadenopathy. On the basis of these imaging features alone, Kaposi sarcoma in this location might be indistinguishable from laryngeal primary squamous cell carcinoma; however, the findings at imaging and at laryngoscopy, in concert with the patient's HIV-positive status, were suggestive of the diagnosis.

clude glomus tumor and myopericytoma (7). Hemangiopericytoma (discussed earlier) was previously included in the category of pericytic tumors but is now considered to be more closely related to solitary fibrous tumors. Thus, this section is focused on sinonasal glomus tumor.

Glomus tumors are rare, accounting for less than 2% of all soft tissue tumors. They are composed of cells that closely resemble the modified smooth muscle cells of the glomus bodies of the dermis (7). These tumors are distinct from and should not be mistaken for the more common head and neck paragangliomas (eg, glomus jugulare, glomus tympanicum, and glomus vagale), which are neuroendocrine tumors derived from the paraganglia of the autonomic nervous system. Glomus tumors occur most commonly in the distal extremities, but sinonasal glomus tumors (also referred to as glomangiopericytomas or sinonasal-type hemangiopericytomas) are well recognized (7,78). Sinonasal glomus tumors are well-delineated but unencapsulated cellular tumors consisting of closely packed cells that form short fascicles, which sometimes exhibit a storiform, whorled, or palisaded pattern, with multiple interspersed vascular channels. These tumors are believed to originate from modified perivascular glomuslike myoid cells in the nasal cavity and paranasal sinuses.

Sinonasal glomus tumors occur in people of all ages, but the peak incidence is in the 7th decade of life, with a slight predominance in females. The tumors are manifested clinically by symptoms of nasal obstruction, epistaxis, difficulty breathing, sinusitis, headache, or nasal congestion. Rare malignant glomangiopericytomas have been reported and are usually characterized by large size (maximum diameters of more than 5 cm) and osseous invasion.

At CT, sinonasal glomus tumors appear as enhancing soft tissue masses. Large tumors may extend into the orbits and intracranial compartment, destroying the adjacent bone. At MR imaging, the tumors usually show signal isointense to that of muscle on T1-weighted images and appear hypo- to isointense relative to muscle on T2-weighted images. After the administration of intravenous contrast material, they typically demonstrate marked enhancement (79) (Fig 19), although the degree of enhancement varies. Larger tumors can demonstrate flow voids (80). Hypervascularity in a sinonasal mass should alert the radiologist to include this entity in the differential diagnosis.

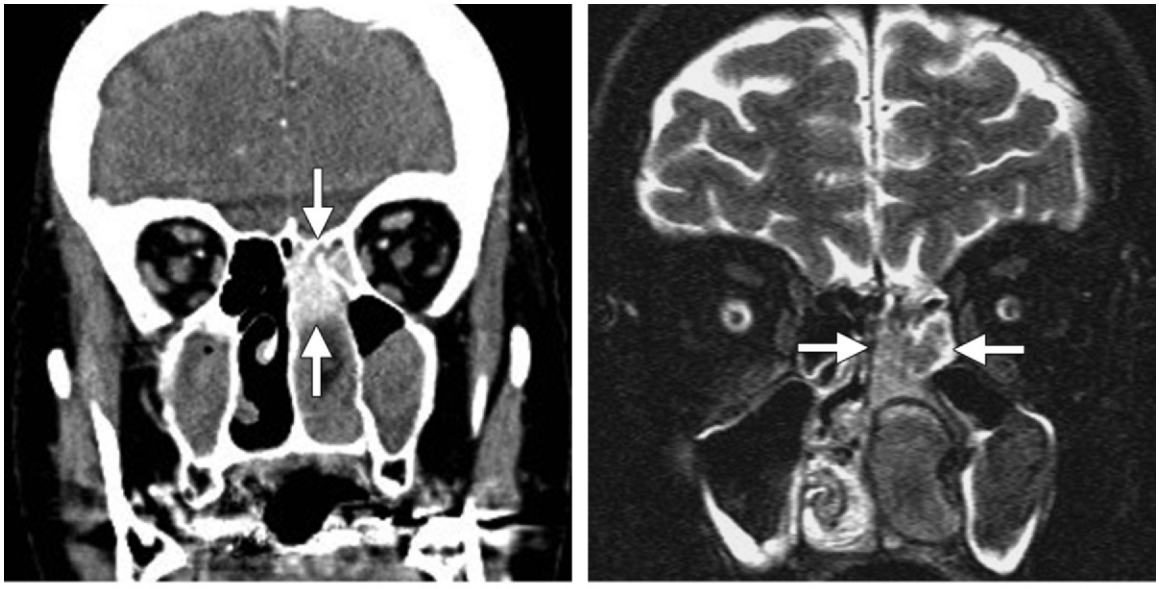

a. b.

**Figure 19.** Sinonasal glomus tumor (glomangiopericytoma). **(a)** Coronal reformatted image from contrast-enhanced CT in an 81-year-old woman with nasal obstruction and anosmia demonstrates an intensely enhancing nasoethmoidal mass (arrows) abutting the anterior skull base. **(b)** Coronal STIR MR image shows that the mass (arrows) has signal intensity similar to that of gray matter. There is a large proteinaceous retention cyst in the nasal cavity, inferior to the mass. **(c)** Axial contrast-enhanced T1-weighted MR image shows marked enhancement of the mass (arrows), a characteristic of sinonasal glomus tumors.

c.

## Chondro-osseous Soft Tissue Tumors

In the most recent version of the WHO classification system, the only benign lesion remaining in the category of chondro-osseous soft tissue tumors is soft tissue chondroma; other benign entities, such as myositis ossificans, have been reclassified. The category also still includes two malignant tumor types: mesenchymal chondrosarcoma and extraskeletal osteosarcoma (7).

### Soft Tissue Chondroma

Soft tissue chondroma (also referred to as chondroma of soft parts) is a benign cartilage-forming tumor that occurs in extraarticular soft tissue. This tumor typically arises in the extremities but rarely is found in the neck, tongue, auricle, cheek, parotid gland, parapharyngeal space, and masticator space (81–83). It is thought that soft tissue chondroma develops from embryonal remnants in areas of preexistent fetal cartilage or that pluripotential mesenchyme differentiates into cartilage as a result of an irritative stimulus. Soft tissue chondromas may occur in people of any age; typically, the tumors are asymptomatic and manifest as slowly growing masses (82).

At CT, soft tissue chondromas appear as circumscribed, heterogeneously enhancing masses. They frequently demonstrate chondroid calcifications (in 33%–70% of cases), which are typically punctate, curvilinear, or ringlike. At MR imaging, the tumors usually have a multilobulated appear-

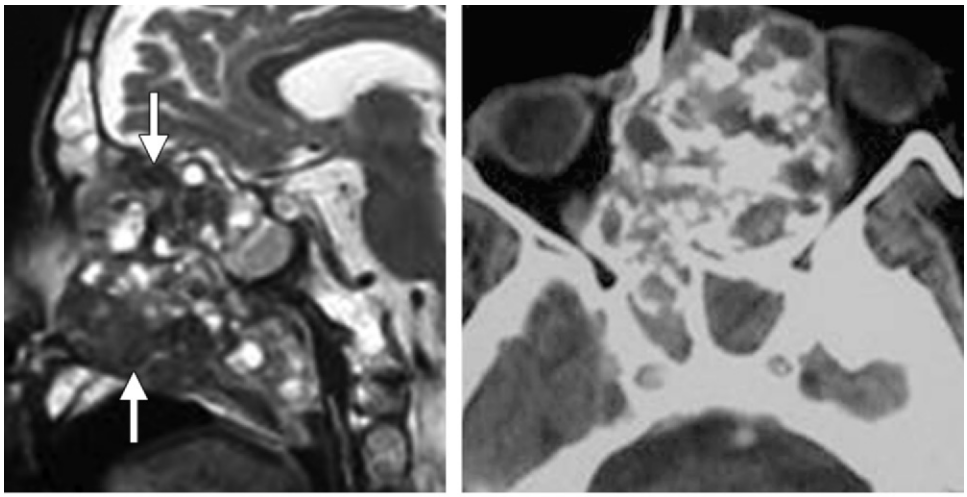

a. b.

**Figure 20.** Chondrosarcoma. **(a)** Sagittal T2-weighted MR image obtained in a patient with a nasal obstruction shows a heterogeneous sinonasal mass with areas of mixed low signal intensity (arrows) due to chondroid matrix calcification. **(b)** Axial CT scan demonstrates coarse chondroid matrix calcification in the tumor, which extends into the left orbit, causing left-sided proptosis.

ance with low to intermediate signal intensity on T1-weighted images, high signal intensity on T2-weighted images, and peripheral or septal contrast enhancement. Chondroid matrix calcifications may be evident at MR imaging as areas of low signal intensity, but these kinds of calcifications are more easily recognized at CT (2,3).

## Mesenchymal Chondrosarcoma

Mesenchymal chondrosarcomas are rare, constituting only 3%–10% of all chondrosarcomas. They may occur at any age, but the peak incidence is in the 2nd and 3rd decades of life. In the head and neck, these tumors arise most commonly in the craniofacial bones. Roughly half of mesenchymal chondrosarcomas are extraskeletal, and the meninges are one of the most common sites of extraskeletal involvement (3,7).

The MR imaging features of mesenchymal chondrosarcoma are variable, but the tumor often appears as a lobulated soft tissue mass with low signal intensity on T1-weighted images, variable and heterogeneous signal intensity on T2-weighted images, and complex heterogeneous enhancement after the intravenous administration of a gadolinium-based contrast material. Chondroid matrix calcifications may be evident at MR imaging as curvilinear or stippled areas of low signal intensity. Plain radiography and CT are particularly helpful for demonstrating these calcifications (3,84) (Fig 20).

## Extraskeletal Osteosarcoma

Extraskeletal osteosarcomas are high-grade malignant tumors that generally occur in an older age group than do osteosarcomas of bone (85). Most head and neck osteosarcomas arise in the mandible or maxilla in people between the ages of 20 and 40 years, whereas the average age of those affected by extraskeletal osteosarcomas is 50 years. Extraskeletal osteosarcomas are extremely uncommon tumors that originate from soft tissue with no attachment to bone or periosteum. In the region of the head and neck, they have been reported to arise in the neck, cheek, parotid gland, scalp, and soft tissues adjacent to the mandible (85,86). Between 5% and 10% of extraskeletal osteosarcomas arise as a direct consequence of irradiation. Trauma is also reported to be a predisposing factor (86).

The MR imaging features of extraskeletal osteosarcomas are nonspecific and vary according to cellular differentiation, the amount of matrix, and the presence or absence of hemorrhage or necrosis. Most extraskeletal osteosarcomas are large at presentation (8–10 cm in diameter) and appear relatively well circumscribed. CT is useful for demonstrating the presence and structure of bone, which in extraskeletal osteosarcomas is characteristically amorphous and, in contrast to the bone in myositis ossificans, is most prominent at the center of the lesion (3,85).

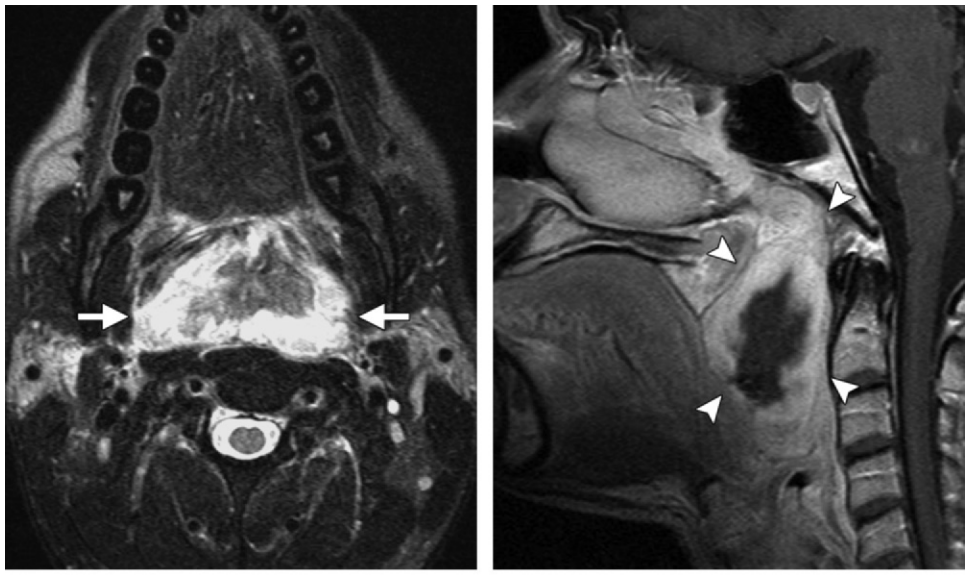

a. b.

**Figure 21.** Synovial sarcoma. **(a)** Axial T2-weighted fat-suppressed MR image (same patient as in Fig 2) shows a mass (arrows) with peripheral high signal intensity and central lower signal intensity, arising from the posterior wall of the oropharynx. Synovial sarcomas frequently exhibit areas with signal hyperintensity like that of fat on non–fat-suppressed images. **(b)** Sagittal contrast-enhanced T1-weighted MR image depicts a peripherally enhancing mass (arrowheads) with a nonenhancing center, a finding suggestive of necrosis.

## Soft Tissue Tumors of Uncertain Differentiation

This category includes tumors that defy histologic classification because of their unclear line of differentiation (7). Myxoma and synovial sarcoma are the most frequently encountered lesions in this group (1).

### Intramuscular Myxoma

Intramuscular myxomas are rare lesions in the region of the head and neck. Most are found in women in the 4th–6th decade of life (87). Myxomas are benign and are characterized by bland spindle shaped cells embedded in hypovascular, abundantly myxoid stroma. Intramuscular myxomas may contain hypercellular areas with increased vascularity; such tumors are described as cellular myxomas (7). Multiple myxomas may be seen in association with fibrous dysplasia in Mazabraud syndrome and may occur also in McCune-Albright syndrome (87). In the head and neck, intramuscular myxomas have been reported to arise in the muscles of the masticator space, scalene muscle, and posterior paraspinal muscles (87,88).

Myxomas are typically well-defined ovoid masses that demonstrate attenuation similar to that of water at CT. At MR imaging, the tumors show signal intensity characteristic of fluid. A peritumoral rimlike feature with signal intensity of fat may be evident on T1-weighted images, and T2-weighted images may show perilesional hyperintensity. These two findings are helpful for distinguishing intramuscular myxomas from other soft-tissue myxoid lesions. Most intramuscular myxomas show some enhancement after the administration of intravenous contrast material (87,88).

### Ossifying Fibromyxoid Tumor

Ossifying fibromyxoid tumor is a slow-growing tumor with intermediate malignant potential, that rarely metastasizes to distant sites. Although these tumors are extremely rare, head and neck involvement is seen in 23% of cases. The tumors are characterized histologically by cords and trabeculae of ovoid cells in a fibromyxoid matrix surrounded by a partial shell of lamellar bone. Ossifying fibromyxoid tumors are often present for years before they are diagnosed (median, 4 years) and are usually between 3 and 5 cm in diameter at presentation. They occur in adults with a median age of 50 years and are more common in men (89).

Head and neck involvement by ossifying fibromyxoid tumors has been found in the neck, sinonasal cavities, oral cavity, scalp, and parapharyngeal space (89). At imaging, the tumors appear as bulky, heterogeneously enhancing masses with peripheral calcification. MR images demonstrate signal isointense to that of muscle on both T1- and T2-weighted images, with central and peripheral areas of lower signal intensity representing areas of calcification on T2-weighted images (3).

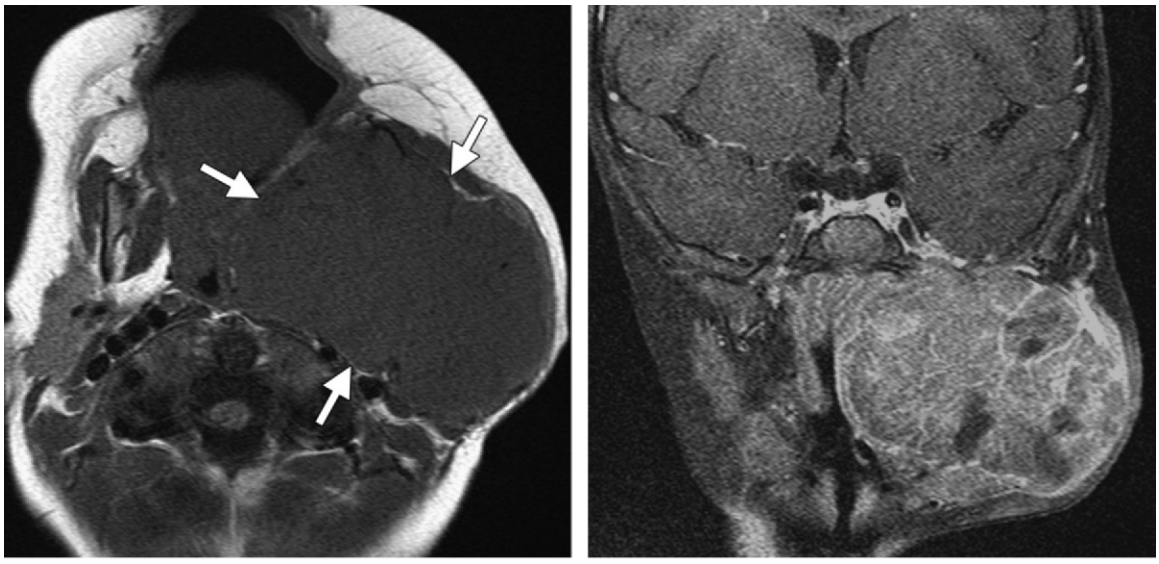

a. b.

**Figure 22.** Ewing sarcoma. **(a)** Axial T1-weighted MR image (same patient as in Fig 1) demonstrates a mass (arrows) with signal intensity similar to that of muscle in the left masticator space. The left mandible has been completely destroyed and is not visible. **(b)** Coronal contrast-enhanced T1-weighted fat-suppressed MR image shows moderate heterogeneous enhancement within the mass.

## Synovial Sarcoma

Synovial sarcomas account for 7%–10% of all sarcomas, with roughly 3% of synovial sarcomas arising in the head and neck region. They occur mainly between the ages of 15 and 40 years and are more common in males. The pharynx (usually the hypopharynx) is the most frequently involved site in the head and neck. Other locations include the masticator space, parapharyngeal space, and sinonasal region. Despite its name, synovial sarcoma does not actually arise from synovial tissue but instead originates from pluripotential mesenchymal cells that display variable epithelial differentiation; for this reason, it has been proposed that the tumor be renamed carcinosarcoma or spindle cell sarcoma of soft tissue (7). These tumors recur in 50% of cases, usually within 2 years after treatment, and they commonly metastasize (40% of cases) to the lungs, bone, and regional lymph nodes (90).

Synovial sarcomas manifest at CT and MR imaging as predominantly solid masses with well-defined smooth margins; infiltration of the adjacent soft tissue is infrequently seen. The lesions may appear either homogeneous or heterogeneous, according to the degree of hemorrhage or necrosis within them. Calcification is seen in approximately 30% of cases (Fig 2) (91). At MR imaging, most synovial sarcomas demonstrate signal that is isointense or slightly hyperintense relative to that in muscle on T1-weighted images and heterogeneously increased on T2-weighted images. T2-weighted images may demonstrate areas of markedly increased signal intensity which may resemble the signal intensity of fat on non–fat-suppressed SE images (91) (Fig 21). Contrast enhancement is variable, but a moderate degree of enhancement is frequently observed (3,90).

## Extraskeletal Ewing Sarcoma and Primitive Neuroectodermal Tumor

Primitive neuroectodermal tumor and extraskeletal Ewing sarcoma are both malignant soft tissue sarcomas that are likely neuroectodermal in origin. Males are affected more commonly than females (92,93). Extraskeletal Ewing sarcoma predominantly affects young adolescents and adults between the ages of 10 and 30 years. Although its occurrence in the head and neck is uncommon, Ewing sarcomas involving the nose, nasopharynx, parotid gland, and cervical soft tissues have been reported. The tumors are aggressive, and their rate of recurrence is high. Distant metastases are common and most often affect the lung. Ewing sarcomas show low attenuation or contain areas with lower attenuation than that in the adjacent muscle at CT, features that correspond with cellular necrosis seen at microscopy. At MR imaging, these tumors generally demonstrate low to intermediate signal intensity on T1-weighted images and high signal intensity on T2-weighted images, and exhibit heterogeneous contrast enhancement (Figs 1, 22). Spontaneous tumoral hemorrhage, adjacent bone destruction, and regional metastatic adenopathy may be demonstrated in some cases (92).

Primitive neuroectodermal tumors have a nonspecific appearance at CT, with low to intermediate attenuation and with no evidence of calcification. Their MR imaging appearance is similarly nonspecific, with low to intermediate signal intensity on T1-weighted images and high signal intensity on T2-weighted images. Areas of hemorrhage are relatively common features. The tumor margins may be relatively well defined, with a pseudocapsule, or may appear infiltrative. MR imaging frequently shows high-flow (low-signal-intensity) vascular channels within the mass, often in peripheral locations (93).

## Conclusions

A wide range of soft tissue tumors may arise in the head and neck region. Although most of these tumors are benign, malignant and locally aggressive soft tissue tumors do occur and can lead to substantial morbidity and mortality. Cross-sectional imaging often plays a key role in establishing a diagnosis and guiding tumor management, with CT and MR imaging both providing useful and complementary data. Because it provides superior soft tissue contrast resolution, MR imaging is best suited for evaluating the extent and internal architecture of these tumors. CT is particularly helpful for evaluating patterns of calcification in some soft tissue tumors and is often the first imaging examination performed when the clinical findings and physical examination are suggestive of the presence of a tumor. The imaging characteristics of many soft tissue tumors are nonspecific, but certain clinical and imaging features of a tumor occasionally are indicative of a tissue-specific diagnosis. Advanced MR imaging techniques may play a role in soft tissue tumor characterization in the future and may lead to an expanded role for radiologists in the diagnosis and management of this diverse group of lesions.

## References


1. De Schepper AM, Bloem JL. Soft tissue tumors: grading, staging, and tissue-specific diagnosis. Top Magn Reson Imaging 2007;18(6):431–444.
2. van Vliet M, Kliffen M, Krestin GP, van Dijke CF. Soft tissue sarcomas at a glance: clinical, histological, and MR imaging features of malignant extremity soft tissue tumors. Eur Radiol 2009;19(6): 1499–1511.
3. Vilanova JC, Woertler K, Narváez JA, et al. Soft-tissue tumors update: MR imaging features according to the WHO classification. Eur Radiol 2007;17(1): 125–138.
4. Walker EA, Song AJ, Murphey MD. Magnetic resonance imaging of soft-tissue masses. Semin Roentgenol 2010;45(4):277–297.
5. Wu JS, Hochman MG. Soft-tissue tumors and tumorlike lesions: a systematic imaging approach. Radiology 2009;253(2):297–316.
6. Miller TT, Sofka CM, Zhang P, Khurana JS. Systematic approach to tumors and tumor-like conditions of soft tissue. In: Bonakdarpour A, Reinus WR, Khurana JS, eds. Diagnostic imaging of musculoskeletal diseases: a systematic approach. New York, NY: Springer, 2010; 313–349.
7. Fletcher CDM, Unni KK, Mertens F. Pathology and genetics of tumours of soft tissue and bone. In: Kleihues P, Sobin LH, eds. World Health Organization classification of tumours. Lyon, France: IARC, 2002.
8. Lloyd C, McHugh K. The role of radiology in head and neck tumours in children. Cancer Imaging 2010;10:49–61.
9. Murphey MD. World Health Organization classification of bone and soft tissue tumors: modifications and implications for radiologists. Semin Musculoskelet Radiol 2007;11(3):201–214.
10. Navarro OM, Laffan EE, Ngan BY. Pediatric soft-tissue tumors and pseudo-tumors: MR imaging features with pathologic correlation. I. Imaging approach, pseudotumors, vascular lesions, and adipocytic tumors. RadioGraphics 2009;29(3):887–906.
11. Robson CD. Imaging of head and neck neoplasms in children. Pediatr Radiol 2010;40(4):499–509.
12. Stein-Wexler R. MR imaging of soft tissue masses in children. Magn Reson Imaging Clin N Am 2009;17 (3):489–507.
13. Subhawong TK, Fishman EK, Swart JE, Carrino JA, Attar S, Fayad LM. Soft-tissue masses and mass-like conditions: what does CT add to diagnosis and management? AJR Am J Roentgenol 2010;194(6): 1559–1567.
14. Razek AA. Diffusion-weighted magnetic resonance imaging of head and neck. J Comput Assist Tomogr 2010;34(6):808–815.
15. Nagata S, Nishimura H, Uchida M, et al. Diffusion-weighted imaging of soft tissue tumors: usefulness of the apparent diffusion coefficient for differential diagnosis. Radiat Med 2008;26(5):287–295.
16. Schnapauff D, Zeile M, Niederhagen MB, et al. Diffusion-weighted echo-planar magnetic resonance imaging for the assessment of tumor cellularity in patients with soft-tissue sarcomas. J Magn Reson Imaging 2009;29(6):1355–1359.
17. van Rijswijk CS, Kunz P, Hogendoorn PC, Taminiau AH, Doornbos J, Bloem JL. Diffusion-weighted MRI in the characterization of soft-tissue tumors. J Magn Reson Imaging 2002;15(3):302–307.
18. van Rijswijk CS, Geirnaerdt MJ, Hogendoorn PC, et al. Soft-tissue tumors: value of static and dynamic gadopentetate dimeglumine–enhanced MR imaging in prediction of malignancy. Radiology 2004;233(2): 493–502.
19. Razek AA, Elsorogy LG, Soliman NY, Nada N. Dynamic susceptibility contrast perfusion MR imaging in distinguishing malignant from benign head and neck tumors: a pilot study. Eur J Radiol 2011;77(1): 73–79.
20. Bastiaannet E, Groen H, Jager PL, et al. The value of FDG-PET in the detection, grading and response to therapy of soft tissue and bone sarcomas; a systematic review and meta-analysis. Cancer Treat Rev 2004;30(1):83–101.

21. Singh HK, Kilpatrick SE, Silverman JF. Fine needle aspiration biopsy of soft tissue sarcomas: utility and diagnostic challenges. Adv Anat Pathol 2004;11(1):24–37.
22. Kilpatrick SE, Cappellari JO, Bos GD, Gold SH, Ward WG. Is fine-needle aspiration biopsy a practical alternative to open biopsy for the primary diagnosis of sarcoma? experience with 140 patients. Am J Clin Pathol 2001;115(1):59–68.
23. Gupta S, Henningsen JA, Wallace MJ, et al. Percutaneous biopsy of head and neck lesions with CT guidance: various approaches and relevant anatomic and technical considerations. RadioGraphics 2007;27(2):371–390.
24. Loevner LA. Image-guided procedures of the head and neck: the radiologist's arsenal. Otolaryngol Clin North Am 2008;41(1):231–250.
25. Brisse H, Orbach D, Klijanienko J, Fréneaux P, Neuenschwander S. Imaging and diagnostic strategy of soft tissue tumors in children. Eur Radiol 2006;16(5):1147–1164.
26. Xi M, Liu MZ, Wang HX, et al. Radiation-induced sarcoma in patients with nasopharyngeal carcinoma: a single-institution study. Cancer 2010;116(23):5479–5486.
27. Cappabianca S, Colella G, Pezzullo MG, et al. Lipomatous lesions of the head and neck region: imaging findings in comparison with histological type. Radiol Med (Torino) 2008;113(5):758–770.
28. Bancroft LW, Kransdorf MJ, Peterson JJ, O'Connor MI. Benign fatty tumors: classification, clinical course, imaging appearance, and treatment. Skeletal Radiol 2006;35(10):719–733.
29. Murphey MD, Carroll JF, Flemming DJ, Pope TL, Gannon FH, Kransdorf MJ. From the archives of the AFIP: benign musculoskeletal lipomatous lesions. RadioGraphics 2004;24(5):1433–1466.
30. Pham NS, Poirier B, Fuller SC, Dublin AB, Tollefson TT. Pediatric lipoblastoma in the head and neck: a systematic review of 48 reported cases. Int J Pediatr Otorhinolaryngol 2010;74(7):723–728.
31. da Motta AC, Tunkel DE, Westra WH, Yousem DM. Imaging findings of a hibernoma of the neck. AJNR Am J Neuroradiol 2006;27(8):1658–1659.
32. Smith CS, Teruya-Feldstein J, Caravelli JF, Yeung HW. False-positive findings on 18F-FDG PET/CT: differentiation of hibernoma and malignant fatty tumor on the basis of fluctuating standardized uptake values. AJR Am J Roentgenol 2008;190(4):1091–1096.
33. Haloi AK, Ditchfield M, Penington A, Phillips R. Facial infiltrative lipomatosis. Pediatr Radiol 2006;36(11):1159–1162.
34. Landis MS, Etemad-Rezai R, Shetty K, Goldszmidt M. Case 143: Madelung disease. Radiology 2009;250(3):951–954.
35. Acar GO, Cansiz H, Acioğlu E, Yağiz C, Dervişoğlu S. Atypical lipomatous tumour of the head and neck region with dyspnea and dysphagia: a case report. Eur Arch Otorhinolaryngol 2007;264(8):947–950.
36. Gritli S, Khamassi K, Lachkhem A, et al. Head and neck liposarcomas: a 32 years experience. Auris Nasus Larynx 2010;37(3):347–351.
37. Spadola L, Anooshiravani M, Sayegh Y, Jéquier S, Hanquinet S. Generalised infantile myofibromatosis with intracranial involvement: imaging findings in a newborn. Pediatr Radiol 2002;32(12):872–874.
38. Kim ST, Kim HJ, Park SW, Baek CH, Byun HS, Kim YM. Nodular fasciitis in the head and neck: CT and MR imaging findings. AJNR Am J Neuroradiol 2005;26(10):2617–2623.
39. Dinauer PA, Brixey CJ, Moncur JT, Fanburg-Smith JC, Murphey MD. Pathologic and MR imaging features of benign fibrous soft-tissue tumors in adults. RadioGraphics 2007;27(1):173–187.
40. Keyserling H, Peterson K, Camacho D, Castillo M. Giant cell angiofibroma of the orbit. AJNR Am J Neuroradiol 2004;25(7):1266–1268.
41. Kokkosis AA, Balsam D, Lee TK, Schreiber ZJ. Pediatric nontraumatic myositis ossificans of the neck. Pediatr Radiol 2009;39(4):409–412.
42. Murphey MD, Ruble CM, Tyszko SM, Zbojniewicz AM, Potter BK, Miettinen M. Musculoskeletal fibromatoses: radiologic-pathologic correlation. RadioGraphics 2009;29(7):2143–2173.
43. Yin B, Liu L, Li YD, Geng DY, Du ZG. Retroperitoneal hemangiopericytoma: case report and literature review. Chin Med J (Engl) 2011;124(1):155–156.
44. Dunfee BL, Sakai O, Spiegel JH, Pistey R. Solitary fibrous tumor of the buccal space. AJNR Am J Neuroradiol 2005;26(8):2114–2116.
45. Kim HJ, Lee HK, Seo JJ, et al. MR imaging of solitary fibrous tumors in the head and neck. Korean J Radiol 2005;6(3):136–142.
46. Park SB, Lee JH, Weon YC. Imaging findings of head and neck inflammatory pseudotumor. AJR Am J Roentgenol 2009;193(4):1180–1186.
47. Narla LD, Newman B, Spottswood SS, Narla S, Kolli R. Inflammatory pseudotumor. RadioGraphics 2003;23(3):719–729.
48. Eskey CJ, Robson CD, Weber AL. Imaging of benign and malignant soft tissue tumors of the neck. Radiol Clin North Am 2000;38(5):1091–1104.
49. Vohra ST, Escott EJ, Stevens D, Branstetter BF. Categorization and characterization of lesions of the orbital apex. Neuroradiology 2011;53(2):89–107.
50. Canale S, Vanel D, Couanet D, Patte C, Caramella C, Dromain C. Infantile fibrosarcoma: magnetic resonance imaging findings in six cases. Eur J Radiol 2009;72(1):30–37.
51. Tanaka T, Kobayashi T, Iino M. Transformation of benign fibrous histiocytoma into malignant fibrous histiocytoma in the mandible: case report. J Oral Maxillofac Surg 2011;69(7):e285–e290.
52. Fritz MA, Sade B, Bauer TW, Wood BG, Lee JH. Benign fibrous histiocytoma of the pterygopalatine fossa with intracranial extension. Acta Neurochir (Wien) 2006;148(1):73–76; discussion 76.
53. Kim KW, Han MH, Park SW, et al. Pigmented villonodular synovitis of the temporomandibular joint: MR findings in four cases. Eur J Radiol 2004;49(3):229–234.
54. Park SW, Kim HJ, Lee JH, Ko YH. Malignant fibrous histiocytoma of the head and neck: CT and MR imaging findings. AJNR Am J Neuroradiol 2009;30(1):71–76.
55. Clark DW, Moore BA, Patel SR, Guadagnolo BA, Roberts DB, Sturgis EM. Malignant fibrous histiocytoma of the head and neck region. Head Neck 2011;33(3):303–308.

56. Leboulanger N, Picard A, Roger G, Garabedian EN. Fetal rhabdomyoma of the infratemporal fossa in children. Eur Ann Otorhinolaryngol Head Neck Dis 2010;127(1):30–32.
57. Defachelles AS, Rey A, Oberlin O, Spooner D, Stevens MC. Treatment of nonmetastatic cranial parameningeal rhabdomyosarcoma in children younger than 3 years old: results from International Society of Pediatric Oncology studies MMT 89 and 95. J Clin Oncol 2009;27(8):1310–1315.
58. Freling NJ, Merks JH, Saeed P, et al. Imaging findings in craniofacial childhood rhabdomyosarcoma. Pediatr Radiol 2010;40(11):1723–1738.
59. Lee JH, Lee MS, Lee BH, et al. Rhabdomyosarcoma of the head and neck in adults: MR and CT findings. AJNR Am J Neuroradiol 1996;17(10):1923–1928.
60. Ramesh P, Annapureddy SR, Khan F, Sutaria PD. Angioleiomyoma: a clinical, pathological and radiological review. Int J Clin Pract 2004;58(6):587–591.
61. Mehta RP, Faquin WC, Franco RA. Pathology quiz case 2: angiomyoma of the larynx. Arch Otolaryngol Head Neck Surg 2004;130(7):889–891.
62. Kim HY, Jung SN, Kwon H, Sohn WI, Moon SH. Angiomyoma in the buccal space. J Craniofac Surg 2010;21(5):1634–1635.
63. Patel SC, Silbergleit R, Talati SJ. Sarcomas of the head and neck. Top Magn Reson Imaging 1999;10(6):362–375.
64. Ramakrishnan VR, Said S, Kingdom TT. Primary leiomyosarcoma of the sphenoid sinus. Arch Otolaryngol Head Neck Surg 2009;135(9):949–952.
65. Fitzpatrick SG, Woodworth BA, Monteiro C, Makary R. Nasal sinus leiomyosarcoma in a patient with history of non-hereditary unilateral treated retinoblastoma. Head Neck Pathol 2011;5(1):57–62.
66. Mulliken JB, Fishman SJ, Burrows PE. Vascular anomalies. Curr Probl Surg 2000;37(8):517–584.
67. Mulliken JB, Glowacki J. Classification of pediatric vascular lesions. Plast Reconstr Surg 1982;70(1):120–121.
68. Dubois J, Alison M. Vascular anomalies: what a radiologist needs to know. Pediatr Radiol 2010;40(6):895–905.
69. Connor SE, Flis C, Langdon JD. Vascular masses of the head and neck. Clin Radiol 2005;60(8):856–868.
70. Ernemann U, Kramer U, Miller S, et al. Current concepts in the classification, diagnosis and treatment of vascular anomalies. Eur J Radiol 2010;75(1):2–11.
71. Moukaddam H, Pollak J, Haims AH. MRI characteristics and classification of peripheral vascular malformations and tumors. Skeletal Radiol 2009;38(6):535–547.
72. O'Regan GM, Irvine AD, Yao N, et al. Mediastinal and neck kaposiform hemangioendothelioma: report of three cases. Pediatr Dermatol 2009;26(3):331–337.
73. Mukerji SS, Osborn AJ, Roberts J, Valdez TA. Kaposiform hemangioendothelioma (with Kasabach Merritt syndrome) of the head and neck: case report and review of the literature. Int J Pediatr Otorhinolaryngol 2009;73(10):1474–1476.
74. Restrepo CS, Martínez S, Lemos JA, et al. Imaging manifestations of Kaposi sarcoma. RadioGraphics 2006;26(4):1169–1185.
75. Venizelos I, Andreadis C, Tatsiou Z. Primary Kaposi's sarcoma of the nasal cavity not associated with AIDS. Eur Arch Otorhinolaryngol 2008;265(6):717–720.
76. Young RJ, Brown NJ, Reed MW, Hughes D, Woll PJ. Angiosarcoma. Lancet Oncol 2010;11(10):983–991.
77. Forton GE, Van Parys G, Hertveldt K. Primary angiosarcoma of the non-irradiated parotid gland: a most uncommon, highly malignant tumor. Eur Arch Otorhinolaryngol 2005;262(3):173–177.
78. Barnes L, Eveson JW, Reichart P, Sidransky D. Pathology and genetics of head and neck tumours. In: Kleihues P, Sobin LH, eds. World Health Organization classification of tumours. Lyon, France: IARC, 2005.
79. Gaut AW, Jay AP, Robinson RA, Goh JP, Graham SM. Invasive glomus tumor of the nasal cavity. Am J Otolaryngol 2005;26(3):207–209.
80. Palacios E, Restrepo S, Mastrogiovanni L, Lorusso GD, Rojas R. Sinonasal hemangiopericytomas: clinicopathologic and imaging findings. Ear Nose Throat J 2005;84(2):99–102.
81. Falleti J, De Cecio R, Mentone A, et al. Extraskeletal chondroma of the masseter muscle: a case report with review of the literature. Int J Oral Maxillofac Surg 2009;38(8):895–899.
82. Kamysz JW, Zawin JK, Gonzalez-Crussi F. Soft tissue chondroma of the neck: a case report and review of the literature. Pediatr Radiol 1996;26(2):145–147.
83. Kwon H, Kim HY, Jung SN, Sohn WI, Yoo G. Extraskeletal chondroma in the auricle. J Craniofac Surg 2010;21(6):1990–1991.
84. Ly JQ. Mesenchymal chondrosarcoma of the maxilla. AJR Am J Roentgenol 2002;179(4):1077–1078.
85. Saito Y, Miyajima C, Nakao K, Asakage T, Sugasawa M. Highly malignant submandibular extraskeletal osteosarcoma in a young patient. Auris Nasus Larynx 2008;35(4):576–578.
86. Hatano H, Morita T, Kobayashi H, Ito T, Segawa H, Hasegawa S. Extraskeletal osteosarcoma of the jaw. Skeletal Radiol 2005;34(3):171–175.
87. Ishoo E. Intramuscular myxoma presenting as a rare posterior neck mass in a young child: case report and literature review. Arch Otolaryngol Head Neck Surg 2007;133(4):398–401.
88. Gandhi MR, Tang YM, Panizza B. Myxoma of the masticator space. Australas Radiol 2007;51(Suppl):B202–B204.
89. Kondylidou-Sidira A, Kyrgidis A, Antoniades H, Antoniades K. Ossifying fibromyxoid tumor of head and neck region: case report and systematic review of literature. J Oral Maxillofac Surg 2011;69(5):1355–1360.
90. Shi H, Wang S, Wang P, Yu Q. Primary retropharyngeal synovial sarcoma. AJNR Am J Neuroradiol 2009;30(4):811–812.
91. Hirsch RJ, Yousem DM, Loevner LA, et al. Synovial sarcomas of the head and neck: MR findings. AJR Am J Roentgenol 1997;169(4):1185–1188.
92. Ng SH, Ko SF, Cheung YC, Wong HF, Jung SM. Extraskeletal Ewing's sarcoma of the parapharyngeal space. Br J Radiol 2004;77(924):1046–1049.
93. Zhang WD, Chen YF, Li CX, Zhang L, Xu ZB, Zhang FJ. Computed tomography and magnetic resonance imaging findings of peripheral primitive neuroectodermal tumors of the head and neck. Eur J Radiol 2011 Feb 26. [Epub ahead of print]

# Soft Tissue Tumors of the Head and Neck: Imaging-based Review of the WHO Classification

*Ahmed Abdel Razek, MD • Benjamin Y. Huang, MD*

**RadioGraphics 2011;** 31:1923–1954 • **Published online** 10.1148/rg.317115095 • **Content Codes:** HN NR OI

**Page 1924**
In the most recent World Health Organization (WHO) system for classification of soft tissue tumors, which was published in 2002, soft tissue tumors are grouped into nine major categories based on their predominant histologic makeup: adipocytic tumors, fibroblastic or myofibroblastic tumors, so-called fibrohistiocytic tumors, smooth muscle tumors, skeletal muscle tumors, vascular tumors, perivascular tumors, chondro-osseous tumors, and tumors of uncertain differentiation (7).

**Page 1924**
One of the major changes in the 2002 update of the WHO classification system was the introduction of two distinct subtypes of intermediate tumors with malignant potential: those with the potential for local invasion, and those with the potential for distant metastasis. Tumors in the first subcategory often recur locally after resection and show an infiltrative and focally destructive growth pattern; however, these lesions do not demonstrate the potential to metastasize. Lesions in the second subcategory are often locally aggressive but also have demonstrated a rare (probability, <2%) but well-documented ability to produce distant metastases (7).

**Page 1926**
Malignant soft tissue tumors usually have low ADC values, which are represented as low signal intensity on ADC maps, whereas benign tumors tend to have higher ADC values. In particular, it has been shown that the ADC correlates with tumor cellularity in soft tissue sarcomas and is lower in malignant nonmyxoid soft tissue tumors than in benign tumors (14–17).

**Page 1929**
Alternatively, a mass at a site that was previously irradiated should arouse concern about the possibility of radiation-induced sarcoma, particularly if the mass occurs years after the completion of radiation therapy. In one study, the average latency period between irradiation for treatment of nasopharyngeal carcinoma and development of a secondary sarcoma in the head and neck was 9 years, with actual intervals ranging broadly from 3 to 26 years (26).

**Page 1931**
Lipomas are the most common mesenchymal tumors, accounting for roughly 16% of soft tissue tumors. Approximately 25% of lipomas occur in the head and neck, mostly in subcutaneous locations at the posterior aspect of the neck.